Title
Going the Distance: Long-Range Conductivity in Protein and Peptide Bioelectronic Materials

Journal
The Journal of Physical Chemistry B, 122(46)

ISSN
1520-6106

Authors
Ing, Nicole L
El-Naggar, Mohamed Y
Hochbaum, Allon I

Publication Date
2018-11-21

DOI
10.1021/acs.jpcb.8b07431

Peer reviewed

THE JOURNAL OF PHYSICAL CHEMISTRY B

Review Article

Cite This: J. Phys. Chem. B 2018, 122, 10403−10423

pubs.acs.org/JPCB

Going the Distance: Long-Range Conductivity in Protein and Peptide Bioelectronic Materials

Nicole L. Ing,[†] Mohamed Y. El-Naggar,[§,∥,⊥] and Allon I. Hochbaum*[,†,‡]

[†]Department of Chemical Engineering and Materials Science and [‡]Department of Chemistry, University of California Irvine, Irvine, California 92697, United States

[§]Department of Biological Sciences, [∥]Department of Chemistry, and [⊥]Department of Physics and Astronomy, University of Southern California, Los Angeles, California 90089, United States

ABSTRACT: Bioelectronic materials interface biomolecules, cells, organs, or organisms with electronic devices, and they represent an active and growing field of materials research. Protein and peptide nanostructures are ideal bioelectronic materials. They possess many of the properties required for biocompatibility across scales from enzymatic to organismal interfaces, and recent examples of supramolecular protein and peptide nanostructures exhibit impressive electronic properties. The ability of such natural and synthetic protein and peptide materials to conduct electricity over micrometer to centimeter length scales, however, is not readily understood from a conventional view of their amino acid building blocks. Distinct in structure and properties from solid-state inorganic and synthetic organic metals and semiconductors, supramolecular conductive proteins and peptides require careful theoretical treatment and experimental characterization methods to understand their electronic structure. In this review, we discuss theory and experimental evidence from recent literature describing the long-range conduction of electronic charge in protein and peptide materials. Electron transfer across proteins has been studied extensively, but application of models for such short-range charge transport to longer distances relevant to bioelectronic materials are less well-understood. Implementation of electronic band structure and electron transfer formulations in extended biomolecular systems will be covered in the context of recent materials discoveries and efforts at characterization of electronic transport mechanisms.

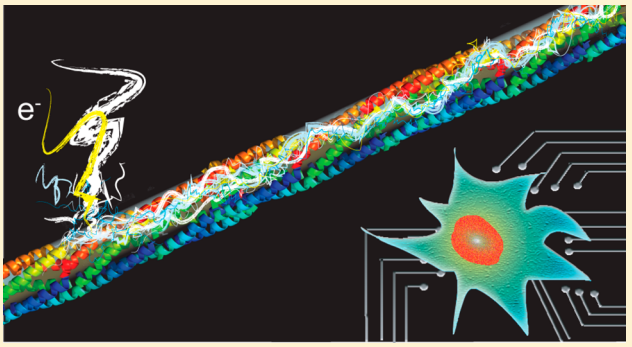

1. INTRODUCTION

Bioelectronic materials interface biology with synthetic devices by interconverting electronic and biological signals and processes. The biological components interfaced to these materials range from biomolecules[1,2] to cells[3,4] and living organisms.[5,6] By seamlessly bridging the synthetic−living interface, without significant perturbation to biological function, bioelectronic materials may improve our understanding of biological systems or even control their functionality. Bioelectronics promise to enhance and prolong human life through biomedical technologies such as implantable power sources,[7,8] wearable sensors,[9,10] therapeutic,[11,12] and prosthetic implants.[13,14] They can also harness functional biological components, such as enzymes, to enhance the sensitivity of nonbiomedical sensors[15−17] as well as improve the efficiency of electrocatalytic syntheses for energy production[18,19] and pharmaceutical applications.[20,21]

Bridging the biotic−abiotic interface is nontrivial, and all the aforementioned bioelectronic technologies will benefit from the development of materials that more seamlessly integrate the two. These materials should be biocompatible and stable under physiological conditions while maintaining effective transduction of electronic and biological signals. For interfacing with organs and tissue, the mismatch in mechanical stiffness between electronic and biological components poses compatibility issues for both wearable and implantable bioelectronic devices.[22−24] For catalysis and sensor technologies, immobilization substrates and techniques can interfere with enzyme functionality.[25−27]

Peptides and proteins are promising building blocks for materials that address these concerns. They are soft materials capable of self-assembling into nanostructures with highly tunable properties,[28−31] including access to a range of dynamic assembly pathways[32] and transient structures.[32,33] Certain peptides and proteins exhibit excellent biocompatibility in terms of eliciting a minimal immune response,[34−36] the ability to be safely degraded/absorbed by the body after use,[37,38] and controllable degradation kinetics.[39−41] Additionally, the chemical diversity of peptides allows for highly optimized enzyme immobilization[42,43] and cellular interfacing.[44−46] Many natural and designed proteins and peptides are also capable of self-assembling into supramolecular nanostructures, such as

Received: August 1, 2018
Revised: September 14, 2018
Published: September 21, 2018

DOI: 10.1021/acs.jpcb.8b07431
J. Phys. Chem. B 2018, 122, 10403−10423

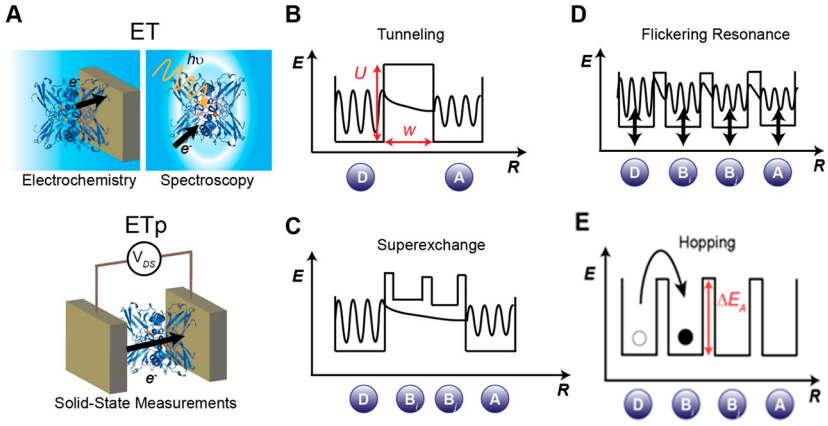

Figure 1. Mechanisms of short-range electronic conduction. (A) Schematic showing ET measurement techniques in electrolyte (top) and solid-state ETp measurements between two electrodes under low pressure or ambient conditions (bottom), with *Pseudomonas aeruginosa* azurin (**PDB 4AZU**). Energy diagrams representing the electron wave function in relation to the donor D, acceptor A, and bridge B states during single-step tunneling (B), superexchange (C), and flickering resonance (D). Energy diagram representing the localization of the wave function or particle-like behavior of the electron during hopping, with an activation energy barrier ΔE_A. (E).

sheets, wires, and tubes.[47,48] The high aspect ratio of these features may offer additional benefits for interfacing with biological components,[49,50] and these dimensions can be achieved without the difficulties and costs associated with many more traditional nanofabrication processes.[51] Lastly, some peptide and protein nanostructures conduct electronic charge and are therefore excellent candidates for bridging the bioelectronic interface.

Electronic conduction across individual peptides and proteins may be categorized either as electron transfer or electron transport[52,53] (Figure 1A) and, for the purposes of this review, will be considered "short-range." Short-range *electron transfer* (ET) refers to the exchange of an electron that occurs as a redox event between an ionically conductive electrolyte and a protein in contact with the electrolyte. Ions in solution screen the change in electric potential during electron transfer events. Conversely, short-range *electron transport* (ETp) refers to the case in which electrons flow through a protein in the absence of electrolyte or electrolyte participation.[52] Short-range ETp therefore requires electron flow across a protein or peptide between two electronically conducting electrodes in the absence of charge-screening electrolyte. Short-range ET and ETp are distinct for several reasons. In short-range ET, electron flow is driven by the difference in the chemical potential (i.e., redox potential) between redox-active species. For short-range ETp between two electrodes of the same material, an externally applied electrical potential difference drives electron flow, and this transport typically occurs under dry or vacuum, as opposed to aqueous, conditions. Short-range ET and ETp are also distinct because ET requires a change in charge state, whereas, for the most part, ETp preserves electroneutrality. Cahen et al. have demonstrated that the primary models used to understand short-range ET are also applicable to short-range ETp through single peptides and proteins.[53]

Although these models were developed for single molecules, it is unclear how these short-range mechanisms extend to transport across longer distances, such as through supramolecular structures. Developing an understanding of the transport mechanisms across supramolecular structures, as opposed to single molecules, is critical to designing better bioelectronic interfaces. Long-range electronic conduction can be formulated in terms of sequential ET processes,[54] but this model invokes strong coupling between electronic states typical of inorganic, not biological, materials. In practice, however, there are many examples of long-range electronic transport through extended supramolecular structures of peptide and protein building blocks.[55−60] The physical mechanisms supporting electronic conduction in these materials are often poorly understood.

In this review, we will discuss examples and mechanisms of electronic conduction occurring over micrometer or longer length scales in supramolecular protein and peptide structures. We will categorize electronic processes at these length scales as "long-range" to distinguish them from the ET and ETp observed through single molecules, which we will refer to as "short-range." We note that single-molecule ETp has been previously identified as "long-range," given the impressive tunneling distances observed through single molecules,[61,62] but such mechanisms over micrometer distances would yield vanishingly small currents inconsistent with experimental observations. As a result, we maintain this distinction, since the operative mechanisms within the two transport distance regimes are likely distinct. Our discussion of short-range ET and ETp through single proteins and peptides will be brief and discussed in the context of building an understanding of longer-range mechanisms. We direct interested readers to several excellent reviews on short-range ET[63−66] and ETp[52,53] through peptides and proteins.

2. MECHANISMS OF SHORT-RANGE ELECTRON CONDUCTION

Short-range (angstrom to nanometer) ET and ETp through peptides and proteins have been extensively studied from both a biological and molecular electronics perspective. Proteins almost exclusively conduct through ET in their native environments, but many of them also support short-range ETp when removed from their natural environments and integrated into solid-state junctions, demonstrating conductivity comparable to conjugated molecules across distances spanning several nanometers.[52,53,67] The solid-state ETp mechanism through a protein need not be the same as its biological ET mechanism, although experimentally, ET and

DOI: 10.1021/acs.jpcb.8b07431
J. Phys. Chem. B 2018, 122, 10403−10423

ETp characteristics are correlated,[68,69] and there is likely a fundamental connection between the two processes.[53]

Short-range ET and ETp in protein and peptide materials can be described using an electron donor (D) and acceptor (A) model, in which D and A can be coordinated metal atoms, amino acids, electrodes, or small organic molecules.[70] We will start by briefly introducing the single-step D-to-A electron transfer process described by Marcus Theory,[71,72] which is the underpinning for the three major ET/ETp short-range mechanisms: superexchange, flickering resonance, and hopping.

2.1. Tunneling. Nonadiabatic tunneling is a single-step electron transfer process between a D and A (Figure 1B). The ET reaction rate k_{ET} depends on $-\Delta G^0$, the driving force for electron transfer between D and A, λ, the total nuclear reorganization energy associated with the electron transfer, and H_{AD}, the temperature-independent tunneling transmission coefficient:

$$k_{ET} = \frac{2\pi}{\hbar(4\pi\lambda kT)^{1/2}} H_{AD}{}^2 e^{-(\Delta G^0+\lambda)^2/4\lambda kT)} \quad (1)$$

In the square barrier tunneling model, the simplest of several empirical barrier models for predicting tunneling transmission,[73−77] H_{AD} is defined by an exponential decay with regard to distance $(R - R_0)$ and has a β decay constant proportional to the barrier height U:

$$H_{AD} = Ae^{-\beta(R-R_0)/2} \quad (2)$$

$$\beta = 2(Um_{eff})^{1/2} \quad (3)$$

$$A = 2U(Um_{eff})^{1/2} \quad (4)$$

where m_{eff} is the effective mass of the electron. Thus

$$k_{ET} \propto e^{-\beta(R-R_0)} e^{-(\Delta G^0+\lambda)^2/4\lambda kT)} \quad (5)$$

The ET rate decays exponentially with the distance between D and A and has a temperature dependence ($k_{ET} \propto T^{-1/2} e^{-\text{energy}/kT)}$), the effect of which is predominantly dependent on the relationship between ΔG^0 and λ. The maximum ET rate is achieved when $\Delta G^0 + \lambda = 0$, at which there is no temperature-dependent activation barrier to transport. Indeed, when ΔG^0 and λ are comparable, k_{ET} is essentially temperature-independent.[54,78] The ET rate is therefore dominated by an exponentially decaying distance dependence, and conductance can be expressed solely as a function of distance[79]

$$G = G_c e^{-\beta R} \quad (6)$$

where G_c is the contact conductance. Gray and Winkler have estimated 20 Å to be the upper limit for efficient biological ET,[80] while Dutton places the limit at 14 Å.[73] Remarkably, ETp tunneling distances up to several nanometers have been experimentally observed. This difference may be attributed to the difference between electron flow in a charge neutral environment and one in which a localized state undergoes a change in the formal charge state, associated with ETp and ET, respectively.[53]

Multistate ET models have been developed to explain biological charge transport occurring over longer distances, such as in respiratory chain complexes. Charge transport in these systems is achieved through chains of redox-active cofactors, conjugated molecules, or metal ions that can act as sites for the formal exchange of localized charge. Adjacent cofactors are situated within tunneling distances to facilitate consecutive tunneling steps or a single tunneling event across several states. These multistate ET models have also been used to describe mechanisms of solid-state ETp through single peptides and proteins,[53] namely, superexchange, flickering resonance, and hopping.

2.2. Superexchange. The superexchange model (SE) is a single-step tunneling mechanism in which there may be multiple bridge states between D and A (Figure 1C). In this mechanism, thermal fluctuations bring the D and A levels into resonance (i.e., the D and A levels become energetically degenerate), causing the electron to tunnel along the bridge states from D to A. The bridge states remain off-resonant during ET, meaning that the electron does not populate the bridge. Rather, the bridge states collectively increase the electronic coupling between D and A, effectively lowering the tunneling barrier. The coupling constant is therefore similar to that of tunneling

$$|H_{AD}|^2 \propto e^{-\beta(R-\Delta R)} \quad (7)$$

where ΔR is the spacing between each state for N states ($\Delta R = R/(N + 1)$). The electronic coupling factor is temperature-independent, but the nuclear factor may have some temperature dependence.[81] SE rates also exhibit an exponentially decaying dependence on distance, albeit slightly weaker than that of tunneling, since the β term for SE is distinct from the square barrier tunneling term (Equation 3).

$$\beta = \frac{2}{\Delta R} \ln\left|\frac{\Delta E_{D/A} - \Delta E_B}{V}\right| \quad (8)$$

The SE decay term scales inversely with between-site spacing and is proportional to the ratio of the energy spacing between the D/A and bridge levels $\Delta E_{D/A} - \Delta E_B$ and the electronic coupling between sites V.[63]

2.3. Flickering Resonance. Beratan and co-workers recently reformulated the discussion of ET, introducing an alternative short-range, single-step transport mechanism known as flickering resonance (FR)[82] (Figure 1D). In FR, the D, A, and bridge sites are simultaneously brought into a temporary resonance. This is distinct from SE, where the bridge states remain off-resonant (unoccupied) during ET, and it is distinct from hopping since the coherence of the wave function is maintained.

FR may be possible when the D, A, and bridge energy levels are similar, such that thermal fluctuations of these states occurs on the same scale as the energy gaps between the states (~tenths of an eV).[83] The vibronic broadening of these energy levels may facilitate a transient and simultaneous alignment between all of the D, A, and bridge states, which would then allow for what Beretan et al. refer to as ballistic charge transfer.[82,83] The ET rate for FR is given by

$$k_{ET} = \frac{2\pi}{\hbar(4\pi\lambda kT)^{1/2}} V^2 P_{match}(2) \quad (9)$$

where $P_{match}(2)$ is the probability of matching between two electronic states, such that the difference between the D and A energy levels is less than the electronic coupling V. Extending FR resonance across multiple states, the probability of matching N site energies decreases multiplicatively by one multiplier per site.[82] In the nonadiabatic limit (specifically, the

DOI: 10.1021/acs.jpcb.8b07431
J. Phys. Chem. B 2018, 122, 10403−10423

case in which coupling energy fluctuations V_{rms} are smaller than site energy fluctuations σ_E) the matching probability $P_{match}(N)$can be expressed as

$$P_{match}(N) \approx e^{-\Phi(R)} \tag{10}$$

$$\Phi = \frac{1}{\Delta R}\ln\left[\sqrt{\frac{\pi}{2}}\frac{\sigma_E}{V_{rms}}\right] \tag{11}$$

Here, the distance between adjacent sites ΔR scales inversely with the total distance of the system, facilitating a weaker distance dependence than tunneling and one similar to that of SE. FR is expected to occur over nanometer-scale distances,[82] although it may have implications for longer-range biological charge transport.[83] Distinct from tunneling, the distance decay exponent Φ has a temperature dependence. Since σ_E increases with temperature and V_{rms} has a weak temperature dependence, the FR decay exponent Φ should increase with temperature, such that the electron transfer rate decays faster with distance as temperature increases.

2.4. Hopping. Hopping is a multistep ET process in which charge is transferred through a series consecutive tunneling events (Figure 1E) (i.e., tunneling between individual and sequential bridge states). In contrast to SE and FR, charge hopping is incoherent, with a localized charge temporarily residing at each site before hopping to the next via oxidation (or reduction). The hopping model is essentially a multistep tunneling model, the efficiency of which is dependent on the driving forces motivating electron flow and the particular arrangement of the redox centers.[62] These redox centers are localized molecular units that can undergo formal electron transfer and the nuclear reorganization associated with a change in charge state. This localization will occur when the Boltzmann probability of occupying a bridge state between D and A exceeds the probability of a single tunneling event between D and A. Since room temperature $kT \approx 26$ meV and a typical protein $\beta \approx 1.2$ Å^{-1},[78] hopping is expected to occur for distances greater than 30 nm and for energy activation barriers $(\Delta E_A) \approx 1$ eV, such that $e^{-\Delta E_A/kT} > e^{-\beta R}$ (Figure 1E).[83]

In this collection of tunneling events, k_{ET} no longer exhibits an exponential dependence on distance, instead varying inversely with the number of hopping steps N and the hopping rate k_N[79,84]

$$k_{ET} \propto k_N N^{-\eta} \tag{12}$$

where η may take on values between 1 and 2.

Hopping has a much stronger thermal dependence than a single tunneling event. Since the wave function is momentarily localized at each state, thermal activation is required to bring the next state into energetic alignment and facilitate the next redox event. Hopping therefore has an exponential temperature dependence that can be expressed in terms of the activation barrier ΔE_A. This is known as an Arrhenius temperature dependence, in which increased temperature facilitates an increase in conduction.[79]

$$G \propto e^{-\Delta E_A/kT} \tag{13}$$

3. MECHANISMS OF LONG-RANGE ELECTRON CONDUCTION

The above short-range mechanisms for single peptides and proteins may have some relevance to electronic conduction on the micrometer-scale through supramolecular assemblies, although the transition from single peptide or protein to multiple peptides or proteins warrants a similar expansion of ET and ETp definitions (Figure 2). As discussed above, for

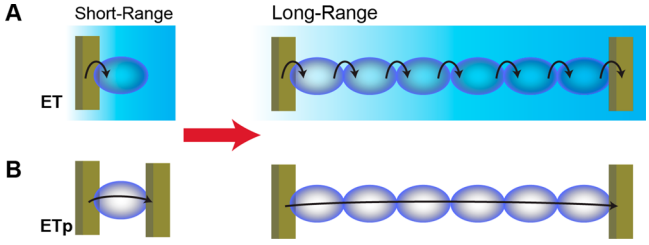

Figure 2. (A) Extending short-range ET through a single peptide or protein to long-range transport through multiple peptides or proteins constitutes a series of short-range ET events. (B) Short-range ETp can be analogously extended to constitute long-range bandlike transport through multiple peptides or proteins.

single peptides and proteins, ET and ETp can be distinguished by the presence or absence of electrolyte participation. Extended to supramolecular or multi peptide/protein systems, long-range ET can be modeled as a series of sequential short-range ET events, such as a series of redox hopping, FR, or SE events, where each event constitutes electron transfer to a nondegenerate energy state (Figure 2A). For a series of adjacent redox hops between discrete, localized states, known as "nearest-neighbor hopping" or thermally activated hopping[54,85,86] (Figure 3A), long-range conductivity σ follows the Arrhenius temperature dependence seen in multistate hopping through a single peptide or protein:

$$\sigma \propto e^{-\Delta E_A/kT} \tag{14}$$

For a series of FR (Figure 3B) or SE (Figure 3C) events, in which hopping occurs between partly delocalized states and is thus considered to be "variable-range",[87−89] conductivity is expected to scale as

$$\sigma \propto e^{-\left(\frac{T_0}{T}\right)^{1/4}} \tag{15}$$

It may be difficult to distinguish between adjacent redox hops between localized states and hops across delocalized states (via a series of FR or SE events), since supramolecular biomaterials are much more sensitive to thermally induced structural changes than the solid materials for which the theory of variable-range hopping was developed. Particularly in the case of FR, the theoretical temperature dependence of Equation 15 may compete with opposite temperature trends associated with Equation 11, convoluting the overall expected temperature-dependent trend. Barring high-resolution structural data over the full range of temperatures tested, it may be difficult to control for structural-induced conductivity changes that may occur over the range of temperatures required to experimentally resolve between thermally activated and variable-range hopping. Nevertheless, the possibility of sequential SE or FR may be inferred if the distances and differences in energy levels between adjacent electronic states are sufficiently small and if kinetic calculations for nearest-neighbor hopping are inconsistent with experimental observations.[83,89]

Conversely, long-range ETp can be analogously defined as continuous electron flow through degenerate electronic states, in which the states may be indistinguishable and take the form

DOI: 10.1021/acs.jpcb.8b07431
J. Phys. Chem. B 2018, 122, 10403−10423

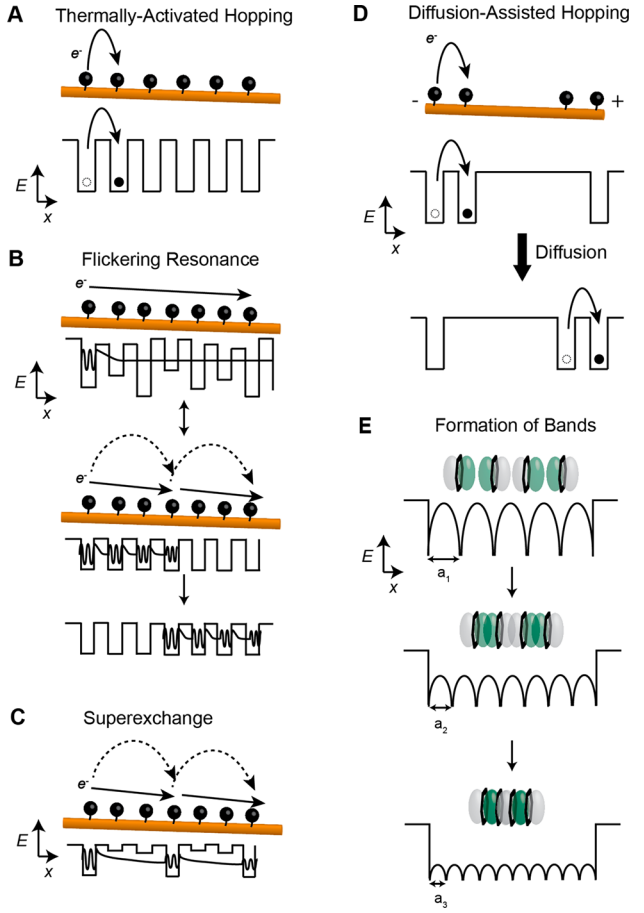

Figure 3. Potential mechanisms for long-range electron transport through peptide and protein supramolecular structures. Redox centers or aromatic moieties may facilitate hopping mechanisms, which can be (A) between adjacent and discrete electronic states, known as thermally activated hopping or between partly delocalized states and occur through a series of (B) flickering resonance or (C) superexchange steps. In each flickering resonance step, thermal fluctuations temporarily bring discrete states into short-lived coherence, and hopping occurs between a series of transient coherent states. Multistep superexchange constitutes a series of tunneling through delocalized states. If the redox centers have some mobility, electron transport may occur through a diffusion-assisted hopping mechanism (E), in which a redox gradient provides a diffusive driving force to assist in hopping over longer distances. (F) Aromatic side chains may also facilitate band formation, given sufficient electronic overlap between adjacent states. Increasing the amount of overlap between aromatic residues lowers the height and width of the barrier between them ($a_1 < a_2 < a_3$), until the barriers effectively disappear at a finite temperature, and a continuous, delocalized band emerges.

of electronic bands (**3.2**) (Figures 2B and 3E). However, this technical distinction has not been established in nomenclature, where terms such as the mitochondrial or photosynthetic "electron transport chain" refer to a series of redox events technically constituting sequential ET processes, as opposed to ETp. Thus, we will focus this review on identifying possible long-range conduction mechanisms, in lieu of a long-range ET versus ETp classification. In this section, we will discuss amino acid-based materials and their potential mechanisms of conduction over long distances (>1 μm).

3.1. Long-Range Conduction via Redox Centers. Extending biological redox-mediated conduction across longer distances (i.e., from nanometers to microns) typically invokes a thermally activated hopping mechanism (Figure 3A), analogous to that observed in short-range ET (Equation 14). However, as discussed above, it may also be possible to achieve this conduction through sequential FR or SE steps, if, for each step, the distance between redox centers is sufficiently short for effective tunneling (≤20 Å) and if the energy levels of the redox centers are similar.[83]

In peptides and proteins, these redox centers may be bound cofactors, the metal centers of metalloproteins, or redox-active aromatic side chains.[73,84] These redox centers can facilitate both short-range and long-range ET by acting as stepping stones for nearest-neighbor hopping, where each step constitutes a redox reaction. While oxidation of the amide bond backbone is highly energetically unfavorable, hemes, iron-sulfur, and copper clusters in metalloproteins have low redox potentials (less than 400 mV vs normal hydrogen electrode (NHE)) suitable for redox reactions in physiological conditions.[90] The oxidation potentials of aromatic amino acid side chains may likewise be suitable for facilitating electron hopping, particularly those of tyrosine and tryptophan,[91−93] with redox potentials ∼1 V versus NHE.[94] Histidine may also potentially function as a redox-active amino acid, with a redox potential ∼1.17 V,[95] although it has been implicated only in poorly efficient ET processes.[93,96] Phenylalanine has recently been proposed as a potential relay amino acid, although the redox potential of alkylated phenyl groups is notably higher ∼2 V.[97] The measured redox potentials and reorganization energies associated with these amino acids are highly sensitive to their molecular and solvent environment.[91] In biological systems, the mechanism of transport through these redox centers is strongly dependent on the formal potential of the chemical substituent. Whereas for formal potentials less than 1 V versus NHE, electron-tunneling events govern long-range transport,[98] hole hopping or electron hopping coupled to proton transfer processes, which reduce the energetic costs associated with a change in charge state, may dominate transport for substituent formal potentials exceeding 1 V versus NHE.[98−103] Although conditions for hole hopping, in particular, are rarely achieved in typical biological systems, it may be a relevant conduction mechanism for bioelectronic materials wired to electrodes poised at arbitrary potentials.

For a material with fixed redox centers, a concentration gradient or electric field can act as a driving force for hopping (Figure 3A), analogous to that observed in redox polymers with discrete redox centers.[104−106] In this model, which has been implicated in biological charge transfer through some bacterial communities,[107−109] a redox gradient (i.e., concentration gradient between oxidized and reduced species) provides the driving force for long-range charge transport. Current across the material can be measured and maximized by situating the material between two electrodes and applying a potential near the formal potential of the redox cofactors. Ions in solution will screen the potential applied across the entire material, but redox centers near the electrodes are capable of direct oxidation or reduction. Consequently, the material will develop a concentration gradient of reduced and oxidized species under steady-state conditions, and this gradient provides a driving force for hopping. In the absence of electrolyte and/or ion screening, an applied electric field can provide the driving force for electron flow across a redox-active material.

If the redox centers have some mobility, either through flexibility of their linker chains or solution solubility, diffusion

DOI: 10.1021/acs.jpcb.8b07431
J. Phys. Chem. B 2018, 122, 10403−10423

may also contribute to the redox gradient and subsequent electron flow[110,111] (Figure 3D). Diffusion-assisted hopping is particularly relevant in cases where the redox centers are spaced too far apart to facilitate consecutive tunneling between adjacent redox sites (thermally activated hopping). The conduction path can be divided into bounded diffusion and hopping components, whereby hopping dominates at high concentrations of redox-active moieties and bounded diffusion dominates at low concentrations. The overall conductivity depends on the concentration of redox sites, as well as the relative time scales of the hoping and physical diffusion processes,[111] and may exhibit a similar temperature dependence as thermally activated hopping.[105]

3.2. Long-Range Conduction via Delocalized States. Long-range conduction can also occur through the formation of bands, electronic states that are delocalized across the entire material. In these delocalized states, the dynamics of charge carriers (electrons or holes) are no longer governed by the discrete state equations described by Marcus Theory (Equation 1). Bandlike conductivity σ is expressed as

$$\sigma = ne\mu \tag{16}$$

where n is the charge carrier density, e is the elementary charge, and μ is the carrier mobility. This formulation describes ohmic carrier transport, in which free (conducting) electrons or holes can be modeled as classical particles moving in continuous bands of delocalized electronic states.

Band formation occurs in crystalline or otherwise highly periodic organic materials. These bands can be considered metallic, semiconducting, or insulating, depending on the band gap energy E_g, that is, the energy required to generate free charge carriers. The electronic properties of conventional solids are determined by E_g near the Fermi level E_F, the energy between the highest occupied and lowest unoccupied states at $T = 0$ K. Metallic conductors have no band gap near E_F, and electrical conductivity scales inversely with temperature (Figure 4A). For semiconductors, $E_g \leq 4$ eV near E_F and

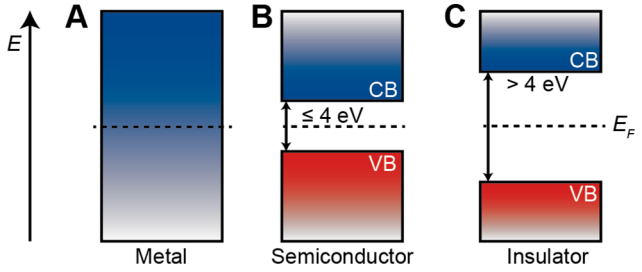

Figure 4. Band diagrams for a (A) metal, (B) semiconductor, and (C) insulator.

electrical conductivity scales with temperature in an Arrhenius dependence, as more free charge carriers are thermally excited from donor/acceptor ionizable impurities and across the band gap[112] (Figure 4B). Although electron hopping conduction also exhibits an Arrhenius dependence, these two mechanisms are distinct in that hopping occurs between localized electronic states, whereas semiconducting transport occurs over a continuum of states delocalized over part or all of the material. If E_g is small (less than 0.2 eV), transport may exhibit little or no temperature dependence near room temperature and a strong temperature dependence, similar to that observed for thermally activated hopping, at low temperatures.[113] If E_g exceeds ∼4 eV near E_F, the material is considered to be electronically insulating (Figure 4C).

In peptides and proteins, the periodicity of the peptide backbone produces band gaps that are calculated to range from semiconducting (≤4 eV) to insulating (>4 eV).[114−116] E_g may be lowered by incorporating aromatic residues to promote delocalization through $\pi-\pi$ orbital interactions, called π-stacking. The resulting electronic orbital overlap contributes to the formation of delocalized states, given that the twist angle and distances between aromatic residues (≤3.4 Å) are optimized.[113] π-Stacking supports semiconducting or metallic-like delocalized electron transport in organic conducting polymers and may facilitate similar transport in peptides and proteins if (1) the distance and torsional angles between neighboring aromatics is sufficient for delocalization between adjacent residues and (2) if the $\pi-\pi$ interactions possess the long-range periodicity required to facilitate delocalization along the length of the supramolecular structure. If π-stacking electronic delocalization is interrupted such that it is insufficient to support bandlike transport over distances between electrodes, thermally activated hopping becomes the dominant transport mechanism between discrete adjacent states (Figure 3A).[117−119] While electron hopping is possible across narrow barriers between delocalized domains, aromatic amino acid side chains may act as intermediate bridge states between these domains to lower the energetics of transport.[92,98] In such cases, this hopping would be analogous to the sequential redox hopping observed in cofactor chains.

FR (Figure 3B) has been proposed as another possible mechanism to form extended bandlike states, as a consequence of short-lived (∼fs) coherences, yet it has not been experimentally verified beyond nanometer distances and may instead may be coupled to a hopping process to achieve micrometer-scale distances.[82,83] Notably, the distance between natural (proteinogenic) aromatic amino acid side chains in folded proteins and peptides typically exceed the 3.4 Å upper limit for efficient π-orbital delocalization,[120−122] making hopping a more likely mechanism for transport through supramolecular peptide and protein structures composed of natural amino acids, provided that the oxidation potentials are suitable to allow efficient multistep hopping, as discussed above. More efficient overlap may be obtained through the incorporation of conjugated small molecules (Section 4.2.1) or non-natural (nonproteinogenic) amino acid side chains (Section 4.2.2).

3.3. Chemical Structure of Peptides and Proteins Affecting Short-Range Electronic Conduction. Chemical features of peptides and proteins reduce the activation barrier to short-range charge transport by variation of the highest occupied molecular orbital (HOMO) and lowest unoccupied molecular obital (LUMO) energies and/or enhancement of intramolecular electronic state coupling.[123−125] Although these contributions have only been demonstrated for single-step tunneling and multistep hopping mechanisms over nanometer-length scales in short-chain peptides, they may have relevance to lowering barriers to long-range transport through a supramolecular system over micrometer-length scales.

Side-chain chemistry strongly affects short-range ET and ETp. Aromatic amino acids, including tryptophan and tyrosine, can enhance ET (or ETp) rates through single molecules by lowering the energy barrier for tunneling and improving electronic coupling to electrode contacts.[124] Tyrosine and tryptophan can also act as redox relay stations to facilitate

DOI: 10.1021/acs.jpcb.8b07431
J. Phys. Chem. B 2018, 122, 10403−10423

biological ET reactions.[99,126,127] Biological ET involving aromatic amino acid oxidation in electrolyte may require the energetic stabilization of coupled proton transfer.[101,128,129] Charged side chains also affect short-range ET and ETp. Protonation of amine side chains has been demonstrated to lower the tunneling barrier for ETp through single peptides.[123,130] For short-range ET mechanisms, in which coordinating ions may affect charge migration, protonation of the amine groups can either increase or decrease the rate of transfer through a single peptide, depending on the Coulombic interactions between charges. Protonation near a positively charged electron acceptor increases the ET rate, whereas protonation near an electron donor, such as tyrosine, which releases a proton during oxidation, lowers the ET rate.[131]

Helical secondary structures, such as α- and 3_{10}-helices, significantly enhance short-range ET and ETp in individual peptides and monolayers. In homopeptides, ETp through a helical configuration is up to 400 times greater than through the equivalent random coil.[123] Density functional theory (DFT) calculations suggest that this difference is due to a decrease in the HOMO−LUMO gap and that torsional angles between amide groups in helical structures enhance electronic coupling through amide bonds along the peptide backbone relative to nonhelical structures.[125]

Secondary structure may also affect short-range ETp and ET by determining the strength of the molecular dipole present along a peptide or protein structure, with the direction of the dipole oriented from the C- to N-terminus. The effect of the dipole is most prominent in helical structures, with the molecular dipole increasing by 5.0 and 4.5 D per residue in α- and 3_{10}-helices, respectively. Conversely, for β-strand structures, the molecular dipole only increases by 0.25 D per residue.[132] Consequently, the dipole moment may significantly improve ET through single α-helical peptides, with an observed 5- to 27-fold increase in ET rate along the dipole (C to N) relative to ET against it (N to C).[133] These directional differences are not observed in random coil peptides, where the net dipole is approximately zero.[134] Spectroscopic studies and ab initio calculations indicate that this dipole moment may also lower the oxidation potentials of amide groups at the C-termini of α- and 3_{10}-helices, potentially facilitating a hopping mechanism through amide groups and hydrogen bonds.[135,136]

4. PEPTIDE AND PROTEIN MATERIALS EXHIBITING LONG-RANGE ELECTRONIC CONDUCTIVITY

In the following sections we discuss examples of supramolecular peptide and protein structures demonstrating long-range electronic conduction. As this field lies at the intersection of electronics and biology, its achievements are motivated from both a molecular electronics perspective and a desire to replicate and understand natural charge-transport phenomena. We will present both biological and synthetic systems composed of natural and unnatural components. It is important to note that the femto- to sub-femtosecond details exclusive to distinct electron transport processes are either difficult or currently impossible to experimentally resolve.[63] Thus, we can only indirectly infer the role of a mechanistic model based on structure and observable parameters, such as the temperature or distance dependence of transport. Moreover, the application of complementary and independent methods of structure and transport characterization is necessary to adequately support a proposed mechanism of conduction. Lastly, it is possible that multiple mechanisms interplay within a particular system, especially under different experimental conditions, and our discussions are limited to identifying the dominant, rather than exclusive, mechanism from available experimental data.

4.1. Cofactor-Based Conductors. In nature, biological long-range electronic conduction primarily occurs through redox chains, such as photosynthetic[137,138] and respiratory systems.[139,140] Conduction via this paradigm is predominantly attributed to electron hopping from cofactor to cofactor along the length of a supramolecular scaffold. The cofactors are typically porphyrins, metal clusters, redox-active small molecules, or redox-active side chains that act as stepping stones for micron-scale transport. As discussed in Section 3.1, the mechanism of transport—multistep tunneling (hopping) or diffusion-assisted hopping—depends on the distances between cofactors. FR may also be a possible long-range transport mechanism, but its role in mediating transport beyond several nanometers remains speculative, and, as discussed above, FR may be coupled to hopping at greater conduction distances.

Long-range transport has been observed in microorganisms, some of which have evolved extracellular respiratory pathways utilizing immobilized redox cofactors capable of delivering current across micrometer distances. One of the most commonly studied species is the anaerobic microbe *Geobacter sulfurreducens* (Figure 5A), which forms electrically conductive

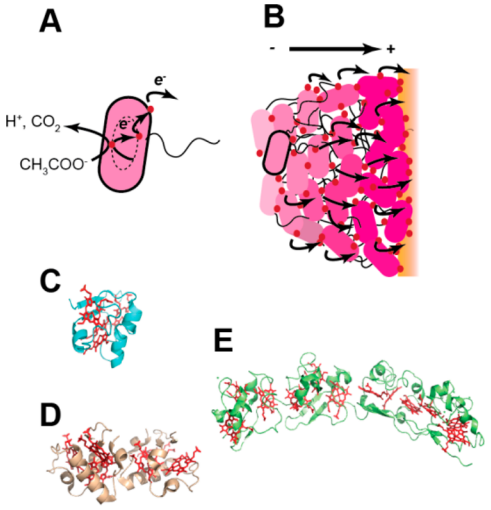

Figure 5. (A) Schematic illustrating *G. sulfurreducens* bacterium metabolism and (B) predominantly redox-gradient-driven electron transport through *G. sulfurreducens* biofilm. Crystal structures of a few of many *G. sulfurreducens* cytochromes: (C) PpcA (**PDB 2LDO**), (D) PpcD (**PDB 3H4N**), and dodecahmeme GSU 1996 cytochrome (**PDB 3OV0**). Heme residues are shown in red.

biofilms (Figure 5B) that have been used in microbial fuel cells to produce electricity from organic material.[141] These biofilms can generate the highest current densities of any monoculture species[142,143] and utilize cytochromes, heme-containing proteins (Figure 5C−E), to facilitate current production.[144,145] In *G. sulfurreducens* biofilms, these cytochromes form a stratified redox gradient to drive hopping charge transport.[107,146] This type of gradient-driven electron transport (Figure 3D) may be a useful motif for bioelectronics

DOI: 10.1021/acs.jpcb.8b07431
J. Phys. Chem. B 2018, 122, 10403−10423

applications, as it has demonstrated energy storage utility in redox-active polymers.[147,148]

These scaffolds have also been replicated in synthetic peptide and protein systems, in which redox-active molecules have been appended to self-assembling peptide and protein sequences to form conductive nanostructures. Inspired by redox-mediated current production in *G. sulfurreducens* biofilms, Altamura et al. created nanofiber films from a chimeric protein composed of an amyloid sequence, known to self-assemble into fibers, and a redox-active protein, rubredoxin (Rd), which contains an $Fe^{2+/3+}$ active site, chelated by four cysteines.[149] The 1 nm distance between iron centers is sufficient for a hopping mechanism (Figure 3A), although the flexibility of the amyloid domain N-terminus, connected to the Rd, permits some mobility of the redox site and therefore suggests some dynamics associated with charge transfer, for which a diffusion-assisted hopping mechanism may be relevant. This flexibility may slightly alter the ET rate relative to more rigidly bound redox centers, but the exact k_{ET} was not measured. Films cast from these fibers exhibited wet conductivities of 3.1 μS/cm and dry conductivities of 2.4 μS/cm, which are comparable to conductivities of peeled *G. sulfurreducens* biofilms.[57] These chimera nanofibers were also able to reduce oxygen via electron transfer from the electrode, along Rd sites and to cross-linked laccase enzyme.

Redox-active protein nanowires have also been demonstrated using diphenylalanine (FF) supramolecular scaffolds (see Section 4.3.2), a sequence motif found in amyloid-forming proteins and capable of self-assembly into nanofibers and nanotubes.[150] By attaching ferrocene onto FF, Wang et al. formed nanowires capable of delivering charge from an electrode to immobilized glucose oxidase. Although the conductivity of FF nanostructures alone ranges from semiconducting[151] to electrically insulating,[152,153] the ferrocene moieties conjugated to the peptide fibers were spaced closely enough to form a redox conduit capable of transporting charge across the fiber scaffolds up to a micrometer in length. While ferrocene is not formally a cofactor for enzyme function, as a coordinated Fe^{2+}/Fe^{3+} center, it is capable of reversible redox reactions and facilitating redox hopping charge transport.

Shewanella oneidensis MR-1 is another well-studied model organism capable of extracellular electron transport to and from[154] solid-state electrodes, including in microbial fuel cells.[155] This functionality relies on structurally and electrochemically characterized multiheme Mtr/Omc cytochrome complexes that span the cell envelope.[156] Long-range cytochrome-dependent transport has also been observed in biological nanowires produced by *S. oneidensis*. Once thought to be primarily protein "pilus-like" fibers,[157] these nanowires were later revealed to be cytochrome-decorated membrane extensions.[158] Nevertheless, these redox scaffold membrane nanowires provide bioinspiration for long-range electron conduction.[159] Electron cryo-tomography reveals that these nanowires are decorated with patches of tightly packed cytochromes (~7−9 nm center-to-center), extending tens of nanometers in length along the nanowires, with interpatch distances exceeding tunneling distances.[110] This structural information suggests that electron transport along the nanofibers is facilitated through a combination of direct hopping events and diffusion-assisted hopping (Figure 3D) between neighboring redox proteins.[111] Recent electrochemical gating measurements of conduction through *S. oneidensis* cells confirm the role of the multiheme conduits in mediating redox transport over micrometer length scales. These measurements also revealed a thermal activation energy in excellent agreement with hopping calculations through the Mtr decaheme cytochromes.[160]

4.2. Hybrid Bio-Organic Proteinogenic and Nonproteinogenic Conductors. Apart from redox-mediated systems, long-range conduction may also be possible through the formation of delocalized states. Since the 3.4 Å packing distance required for efficient delocalization is difficult to achieve with proteinogenic amino acid side chains, multiple studies have swapped natural aromatic side chains for nonproteinogenic ones or have used peptides as a supramolecular scaffold to guide conjugated small molecule packing.

The mechanism of long-range transport through delocalized states is highly dependent on the degree and length of conjugation. If the conjugation axis is persistent along the length of the supramolecular structure, potentially forming delocalized states, transport can be metallic-like or semiconducting. The type of bandlike conduction in these systems is determined by observing the relationship between temperature and conductivity. For metallic-like conductors, temperature scales inversely with conductivity, as increasing temperature reduces carrier mobilities; for semiconductors, conductivity scales with temperature, due to thermal excitation of charge carriers. If conjugation is restricted to localized regions along the supramolecular structure, hopping may be required for micrometer-scale transport. This hopping mechanism would be akin to the sequential reduction and oxidation events observed in redox-mediated hopping and would therefore also exhibit a temperature-dependent conductivity. Since semiconducting and hopping behaviors both have an Arrhenius temperature dependence and their conductance scales inversely with length (Pouillet's law), a crystal structure and/or spectroscopic evidence may be required to demonstrate the electronic delocalization that would distinguish the two. For a delocalized system, temperature-dependent conductivity measurements can be used to distinguish between metallic-like versus semiconducting transport. Hall-effect measurements may also be a valuable tool in distinguishing between band and hopping carriers, since hopping charges in organic semiconductor films will drift in an opposite direction to band carriers subject to an orthogonal magnetic field.[161] Hall-effect measurements may be particularly useful, since thermal disorder can compete with π-stacking interactions and simultaneously induce both band and hopping transport in organic semiconductors.[161]

4.2.1. Hybrid Bio-Organic Proteinogenic Conductors. The molecular and organic electronics community has pursued peptide−small molecule conjugates for the formation of self-assembling organic conductors. Amino acids are an ideal candidate to merge with conjugated molecules, since they offer both water solubility and a self-assembly pathway for the formation of electronically delocalized nanostructures. These systems typically incorporate short peptide sequences predisposed to form supramolecular structures, such as coiled-coils, β-sheets, α-helices, collagen, or elastin mimics.[162] Some notable conjugates include oligothiophenes,[163,56,164−166] naphthalene diimides (NDI),[167−169] perylene diimides,[169−174] and fluorenyl-9-methoxycarbonyl (Fmoc).[55,175,176]

These conjugates may facilitate long-range ETp through the formation of delocalized states. The nature of interstate coupling, in these cases $\pi-\pi$ interactions, determines whether bandlike transport has a metallic-like or semiconducting

DOI: 10.1021/acs.jpcb.8b07431
J. Phys. Chem. B 2018, 122, 10403−10423

temperature dependence (Section 3.2). However, if the aromatic residues are spaced too far apart to form delocalized states, or if the delocalization lengths are broken by molecular distortions, long-range ETp may occur through thermally activated electron hopping, analogous to that observed with redox cofactors (Section 4.1).

Design considerations in this paradigm are especially critical, given that a peptide's intermolecular hydrogen-bonding network can directly influence the geometry, and therefore the degree and direction, of intermolecular $\pi-\pi$ interactions.[177] Govindaraju et al. created two dipeptide-conjugated naphthalene diimides: one with a nonproteinogenic amino acid, 2-aminoisobutyric acid, Aib-Aib, and the other with a natural amino acid, Ala-Ala, with Aib only differing from Ala by an extra methyl group.[178] However, the two dipeptides are known to adopt either helical or β-sheet structures, which, in turn, resulted in two distinct nanostructures with different conductivities. The Aib-Aib NDI-conjugate formed one-dimensional (1-D) nanotapes with a cofacial orientation of the NDI groups and a conductivity of 3.5×10^{-6} S/m, while the Ala-Ala NDI conjugate formed two-dimensional (2-D) nanosheets with an edge-to-edge (coplanar) NDI orientation and less than half the conductivity, 1.6×10^{-6} S/m. Indeed, Tovar et al. have shown that modest changes to a peptide sequence can result in vastly different electronic coupling regimes: disordered excimeric structures (a dimeric species associated in a short-lived excited electronic state[179]) or ordered electronically coupled states.[178] The operative conduction mechanism in each regime may be distinct, as ordered electronically coupled states facilitate a metallic or semiconducting bandlike transport, whereas disordered excimeric structures conduct through hopping between localized states.

Although hydrogen bonding plays a significant role on the resultant hybrid structure, it cannot be the only factor driving structural formation if delocalization is to be preserved. These periodic $\pi-\pi$-interactions require[183] that the conjugated component contribute to the assembly and structural stability of the hybrid nanostructure, since assemblies exclusively stabilized by β-sheet hydrogen bonds have intermolecular distances (typically ~4.7 Å) that preclude efficient orbital overlap (3.4 Å).[180,181] The β-sheet secondary motif is commonly used in polymer–peptide conjugates due to its tendency toward strong intermolecular aggregation.[182] Work by Bäuerle et al.[166] demonstrates the importance of tempering the dominance of peptide hydrogen bonding. They designed two conjugated systems combining a quaterthiophene derivative, tetra(3-hexylthiophene) (T) with peptide sequences (P) known to form β-sheet domains, in both a T-P diblock oligomer and a P-T-P configuration. Although these structures formed nanofibers in organic solvent, assembly was dominated by β-sheet hydrogen bonding, as opposed to $\pi-\pi$ interactions, and electronic delocalization was not observed in either arrangement. Conductance measurements were not performed, albeit low conductivities would be expected in the absence of π-stacking.

Several approaches have been used to preserve π-stacking interactions in peptide–conjugate hybrid systems. Stupp et al. achieved delocalized hybrid nanostructures by creating a bolaamphiphile.[165] Bolaamphiphiles differ from single-headed amphiphiles in that they have hydrophilic groups flanking a sufficiently long hydrophobic chain; their design can be dissected into three parts: polar amino acids at the ends for solubility, structure-forming amino acids for assembly, and an aromatic core for conductivity. A quinquethiophene molecule was chosen as the center segment, and alkyl spacers were added to confer flexibility, which allowed for simultaneous π-stacking and hydrogen bonding in the resultant hydrogel. Conductance measurements were not performed, but circular dichroism and absorption/emission measurements suggest the presence of π-stacking between bolaamphiphile building blocks.

Hodgkiss et al. developed nanofibers using two different modes of attachment to a perylene dimide core.[171] In the "forward-attached" case, a self-assembling β-sheet peptide sequence was attached using a glycine linker at the N-terminus, while in the "reverse-attached" case, the peptide sequence was attached using an ethylamino linker at the C-terminus. In the forward-attached design, the peptide backbone extends N to C away from the core, while in the reverse-attached design, the peptide backbone extends C to N away from the core. These two designs gave nanofibers with distinct aqueous spectral profiles: the forward-attached peptide conjugate exhibited strong coupling between delocalized π-orbitals (consistent with H-aggregation), while the reverse-attached peptide conjugate exhibited a spectral signature suggestive of a rotational offset between the perylene units. Upon solid-state gating, films of forward-attached nanofibers exhibited weak semiconducting p-type behavior (majority of charge carriers are mobile holes), which was unexpected given the n-type behavior (majority of charge carriers are mobile electrons) associated with perylene materials and the high electron affinity of the perylene core. This unexpected change in electronic structure is likely due to the integration of the peptide, but electronic structure calculations, such as DFT, were not performed to validate a mechanism for the charge carrier polarity inversion. Although electronic measurements were not performed on the reverse-attached peptide, the lack of delocalization implies that any conductivity in the system would be mediated through hopping and would have significantly lower values than the delocalized forward-attached peptide system, due to weaker electronic coupling.

Tovar et al. have developed several π-conjugated peptide nanostructures by directly embedding the conjugated unit into the peptide backbone. In this design, they have flanked oligothiophenes,[68,69,82,83] diacetylene (later photopolymerized into polydiacetylene),[185] naphthalene, perylene,[169] and other aromatic compounds[186] between two β-sheet forming peptides to create water-soluble peptide–conjugate building blocks. This design encourages the aqueous self-assembly of ribbon and gel structures, which, on a molecular level, promote cofacial aggregation of the conjugated organic compounds.[163,169] Upon gating, films of these nanostructures exhibited hole mobilities as high as 1.7×10^{-2} cm^2 V^{-1} s^{-1} for quaterthiophene-containing peptides[184] and 3.8×10^{-5} cm^2 V^{-1} s^{-1} for sexithiophene-containing peptides.[186] Notably, the best-performing quaterthiophene-peptide variant demonstrated mobilities comparable to those observed in films of quaterthiophene derivatives not bound to peptides,[187] suggesting that the presence of peptide in this system did not adversely affect conductivity. Spectroscopic evidence for delocalization suggests that these materials are bandlike conductors and that their ability to gate conductivity electrostatically is a characteristic feature of semiconductor band transport. Tovar and co-workers have also developed a straightforward solid-phase resin synthesis to incorporate

DOI: 10.1021/acs.jpcb.8b07431
J. Phys. Chem. B 2018, 122, 10403–10423

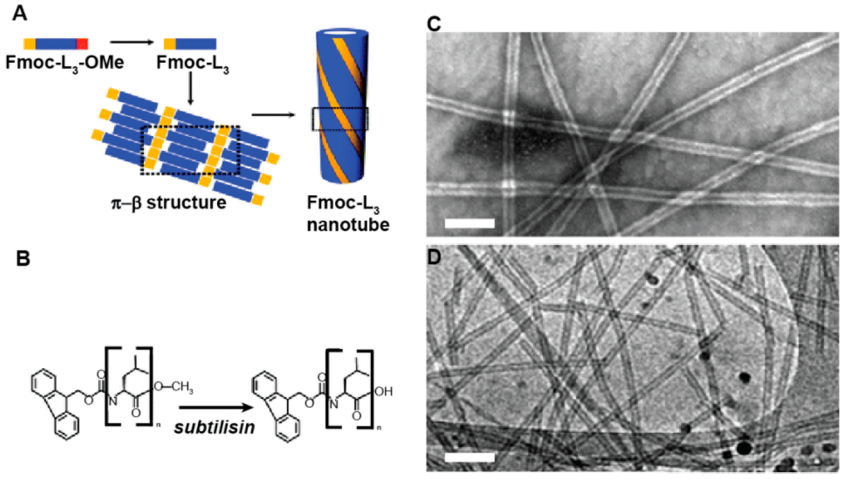

Figure 6. (A) Scheme for self-assembly of nanotubes assembly of Fmoc-L_3, which is converted from Fmoc-L_3-OMe via enzymatic hydrolysis (B). (C) Transmission electron micrographs of nanotube structures stained with 2% uranyl acetate and (D) AFM images of nanotubes on mica. Scale bars are 100 nm. Adapted from Xu et al.[55] with permission from the Royal Society of Chemistry. Copyright 2010. https://pubs.rsc.org/en/content/articlelanding/2010/nr/b9nr00233b#!divAbstract

commercially available semiconducting and fluorescent chromophore units into oligopeptide backbones, bypassing many synthetic and solubility hurdles with creating semiconducting small molecule–peptide conjugate materials.[169,186]

Another approach has been to incorporate aromatic moieties to the N-terminus of hydrophilic peptides (or single amino acids), creating amphiphilic peptide systems.[162,168,175,188,189] On the basis of structural studies on Fmoc-diphenylalanine (FF), Ulijn et al. have proposed that these amphiphile peptide systems form $\pi-\pi$ interlocked β-sheets.[79] The same group measured the conductivity of conjugates with Fmoc appended to a leucine tripeptide (Fmoc-L_3)[55] (Figure 6), which, of the several amphiphile variants tested, demonstrated the most electron delocalization, according to fluorescence measurements.[189] The resulting π-stacked β-nanotubes had minimum sheet resistances of 0.1 MΩ/sq in ambient conditions. Although this conductivity value is low compared to conjugated polymer films, these peptide amphiphile systems have the unique feature of enzyme-triggered assembly (Figure 6A,B), which may allow for better reproducibility and control over the self-assembly process.[190] Access to tunable kinetic control potentially expands the functional applications of these conductive materials, as enzyme-mediated assembly of the conjugated materials have demonstrated refuelable assembly and disassembly kinetics that may be particularly useful for reconfigurable biointerfacing applications.[33,191] Red-shifts in the fluorescence spectra of assembled gels suggest they form delocalized structures, and, as with other π-stacked systems in this classification, these amino acid conjugates are expected to be semiconducting.

4.2.2. Conductive Peptides Incorporating Nonproteinogenic Amino Acids. Since aromatic delocalization is difficult to achieve using natural amino acids, Ashkenasy et al. have attempted to restore π-stacking in pure amino acid systems by developing a new category of amino acid conductors, in which natural amino acid side chains have been replaced by small aromatic compounds. They have demonstrated nanotubes with delocalized states by adding NDI side chains to otherwise electronically insulating[192−194] cyclic D,L-α-peptide nanotubes[195,196] (Figure 7). Cyclic D,L-α-peptides, although less promiscuous than their linear counterparts, have a lower

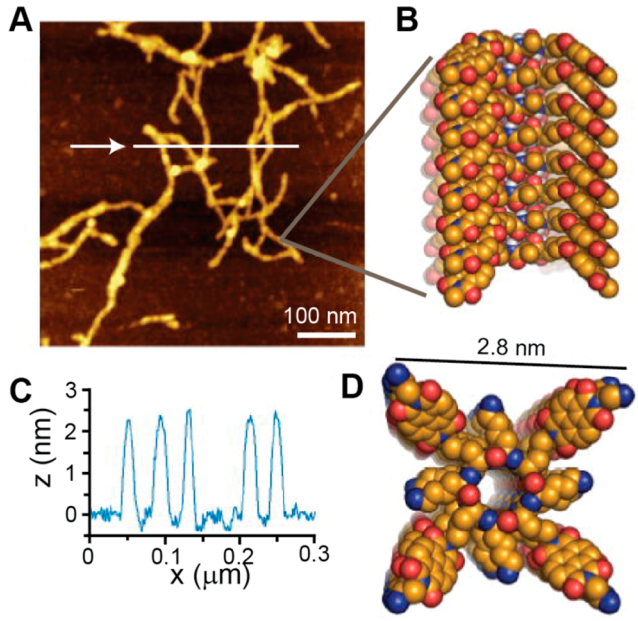

Figure 7. (A) AFM image of peptide fibers formed from cyclic nanotubes on mica. (B) Suggested space-filling model for self-assembled cyclic peptide. The lateral cross section determined by topographical height profiles (C) is consistent with the diameter of the peptide nanotube (D). Reproduced with permissions from Ashkenasy et al.,[195] copyright 2005 Wiley-VCH Verlag GmbH & Co. KGaA https://onlinelibrary.wiley.com/doi/abs/10.1002/smll.200500252.

entropy that tends to a greater degree of control and predictability[197] over their nanotubular self-assembly[195,196] (Figure 7A). In nanotubes, the aromatic structures adopt a tilt with an interaromatic distance of 3.6 Å, thereby facilitating intermolecular electronic delocalization[195] (Figure 7B). Subsequent studies with cyclic D,L-α-peptides, with both natural amino acid side chains and napthyl substituents, suggest proton, rather than electron, hopping to be the dominant transport mechanism in dehydrated and hydrated environments.[198] In dehydrated films, aromatic stacks provide proton channels, promoting proton conductivity through

DOI: 10.1021/acs.jpcb.8b07431
J. Phys. Chem. B 2018, 122, 10403−10423

hydrogen bonding. In hydrated films, a water adlayer on the surface of the peptide facilitates proton conduction, wherein proton-donating carboxylic acid side chains become important for conductivity. Although the electronic conductivity in these systems is very low (with the greatest contribution being less than or equal to 20% of total current, achieved under vacuum conditions), proton conducting materials have potentially useful applications and represent a common biological charge transport mechanism.[199−202]

Proton involvement in these systems may suggest a hopping mechanism, in which protons stabilize electron transfer, such as at low relative humidity. As discussed in Section 3.3, protons may be essential in assisting short-chain redox reactions involving aromatic amino acids.[101,129] Nevertheless, the minor role of electronic transport through this system is difficult to characterize, since a predominant hopping mechanism suggests the presence of discrete states, whereas the observation of delocalization suggests a continuum of states. However, such a conflict is not entirely surprising, since the dominant charge carriers are protons, as opposed to electrons, and are governed by a different set of transport mechanisms. Proton conduction mechanisms are beyond the scope of this review, but we direct interested readers to several excellent reviews on the subject.[203−205]

The Ashkenasy group has also incorporated nonproteinogenic aromatic side chains into fiber-forming amyloid β sequences. They formed spectroscopically delocalized states in amphiphilic Glu-Phe dyad fibers by replacing, in each peptide sequence, two phenylalanine residues with two diaminopropionic acids bearing NDI side chains.[206] In another amyloid-β-derived sequence,[207] they showed enhanced nanotube film conductivity when replacing the FF domain with two non-natural 2-thienylalanine (2-Thi) amino acids, achieving pS conductances under low-pressure conditions.[93] Although these conductances are low, further investigation suggested a strong proton contribution to conductivity, based on observations of increasing conductance with increasing relative humidity.[208] From these humidity studies, Ashkenasy et al. concluded that, below 60% relative humidity, conduction was mediated through both electrons and protons (1:2 ratio, respectively), while at high humidity, conduction (increased to the order of nS) was mediated by protons. Nevertheless, these humidity studies were not conducted with Pd hydride electrodes, which are typically used to demonstrate proton conductivity, making it difficult to distinguish changes in conductivity due to proton conduction from those induced by humidity-dependent structural or morphological changes.

4.3. Conductive Peptides and Proteins Composed of Proteinogenic Amino Acids. *4.3.1. π-Stacked Peptides and Proteins.* Long-range electron transport through natural amino acids is nontrivial, as it is difficult to achieve efficient packing distances using natural side chains. Protein nanofibers produced by the *Geobacter* species may be an exception, although the presence of delocalized states remains a point of great interest and contention.[57,209,210,108,211,212] As with nonproteinogenic side chain and peptide−conjugate hybrid structures, long-range conduction in proteinogenic, π-stacked systems could occur through metallic-like or semiconducting bands, given sufficient overlap and carrier injection via redox reactions or electrostatic gating. If π-stacking is not sufficient for complete delocalization along the length of the fiber, long-range transport may occur through hopping between localized low-energy states.

Although live *G. sulfurreducens* biofilms primarily demonstrate long-range, redox-mediated electron transport (section 4.1), conductive nanofibers isolated from *G. sulfurreducens* cultures demonstrate micrometer-scale conductivity[210,213] that is facilitated entirely by natural amino acids. These nanofibers are presumably composed of the structural protein PilA, which is over 85% α-helical in nature[214] (Figure 8A) and is arranged

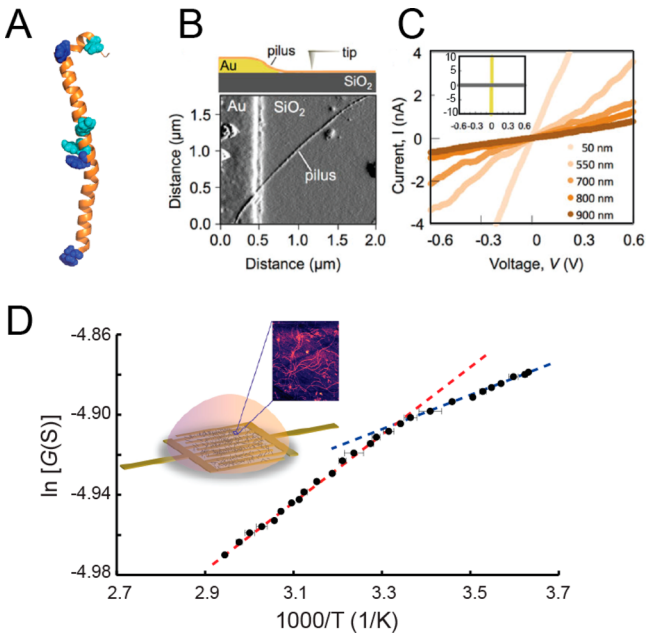

Figure 8. (A) Homology model for *G. sulfurreducens* PilA, with aromatic residues highlighted in blue (PDB 2M7G). (B) Schematic (top) and AFM amplitude image (bottom) illustrating two-point conductive probe measurements on *G. sulfurreducens* nanofiber (pilus) contacting gold electrode. (C) Representative $I-V$ measurements of single nanofiber at various distances from the electrode. (inset) $I-V$ plots of gold electrode (yellow) and silicon background (gray). (D) Temperature-dependent conductivity characteristics of a film of conductive *G. sulfurreducens* nanofibers (schematic, inset) conducted in aqueous environment. Dotted lines show two different regions of liner temperature dependence. Adapted from Lampa-Pastirk et al.[210] © 2016 under Creative Commons License 4.0, Nature Publishing Group https://www.nature.com/articles/srep23517 and Ing et al.[145] with permission from the PCCP Owner Societies.

into supramolecular helical coils via a complex, membrane-associated secretion system.[215] The nanofiber conductivity is exceptionally high compared to many π-stacked amino acid-based nanofibers, with single fiber values ranging from 50 to 5 S cm^{-1}[210,213] (Figure 8B) and comparable to organic metals.[209]

Although cytochromes play a key role in electronic transport through respiring *Geobacter* biofilms (Section 4.1) and bacterial appendages produced by *S. oneidensis*[157,158] (Section 4.1), conduction through these nanofibers does not exhibit signatures of redox-mediated conduction.[216] Reguera et al. have demonstrated that the diffusion-assisted redox conduction observed in live *G. sulfurreducens* biofilms is not contradictory with the presence of intrinsically conductive pili produced by bacteria within the biofilm.[217] Their work suggests that conduction through a network of these nanofibers becomes a significant contributor for biofilm exceeding 10 μm in thickness.

DOI: 10.1021/acs.jpcb.8b07431
J. Phys. Chem. B 2018, 122, 10403−10423

Conductivity in these *G. sulfurreducens* nanofibers increases with decreasing temperature[57,145] (Figure 8C), suggestive of a nonhopping mechanism. Reguera et al. have observed an opposite temperature dependence when comparing single fiber measurements at room temperature versus 77 K.[210] Although this measurement is suggestive of hopping, it is likely that, as with other soft materials, different conduction mechanisms are relevant for different temperature ranges. Thus, a thermally activated mechanism under cryogenic conditions need not be inconsistent with nonthermally activated conduction at much higher temperatures. Malvankar et al. measured a crossover temperature $\approx$ 260 K for conductivity of these nanofiber films.[57] Above 260 K, conductivity increased exponentially upon cooling, whereas below 260 K, conductivity decreased exponentially upon heating. This exponential dependence and crossover have also been observed in organic metals[218] and were attributed to reduced phonon scattering in metallic-like band transport above the transition temperature and trap localization below it.[57] In an aqueous environment and over a physiologically relevant range of temperatures (275 to 338 K), Hochbaum et al. measured a much weaker exponential temperature dependence composed of two regimes[145] (Figure 8D). This weak temperature dependence may be a result of temperature-dependent conformational changes in the protein nanofibers. The authors suggested a possible FR mechanism, since thermal disorder can diminish the probability of coupling between electronic states.[82,83] However, since FR has not been demonstrated over the micrometer distances associated with single nanofibers, any FR mechanism would likely be coupled to hopping, which has an opposite temperature dependence. Because it is unclear whether temperature-dependent conductivity would be dominated by a reduction in thermal disorder or hopping, the role of FR in *Geobacter* nanofiber conduction remains speculative. Measurements performed by these three groups were all done under different environmental conditions and may thus be linked to different mechanisms. Regardless of the conduction mechanism in these nanofibers, a chemical or structural basis for the observed conductivity remains elusive.

Lovley, Malvankar, and co-workers have attributed the conductivity in these bacterial nanofibers to metallic band formation due to the π-stacking of aromatic side chains,[57,209,219,220] though this claim has been heavily contested by other groups.[210,214,221] Powder X-ray microdiffraction of purified *G. sulfurreducens* nanofibers showed a 3.2 Å peak, which was attributed to aromatic stacking of phenyl rings, as these peaks were not present in nanofibers purified from a mutant expressing PilA lacking key aromatic residues.[209] Several homology models based on sequence similarities to such cellular appendages in other microbial species have been invoked to justify the interaromatic distances in *G. sulfurreducens* nanofibers. The sum of the homology models and one docking model, assembled by docking PilA monomers, present conflicting conclusions as to the possibility of π-stacked delocalization along the nanofibers.[209,219,222,221,214,223] Verification of π-stacking is contingent upon obtaining a direct atomic structure model of the *G. sulfurreducens* nanofibers, and spectroscopic evidence of electronic delocalization has yet to be demonstrated.

Nevertheless, modifications to the PilA sequence suggest that the conductivity is sensitive to changes in the aromatic amino acid content. Lovley and co-workers showed that the conductivity of conductive *G. sulfurreducens* nanofibers decreased appreciably when five aromatic amino acids in the PilA sequence were mutated to aliphatic side chains (Ala),[220] with single fiber conductivity measurements suggesting a 3 orders of magnitude decrease relative to wild type (WT) protein (38 ± 1 μS cm^{-1} compared to 51 ± 11 mS cm^{-1}).[191] These findings were corroborated by Reguera et al., who found that a single replacement of one of the tyrosine residues with an alanine residue in the PilA sequence resulted in a sixfold decrease in conductivity, from 4.7 to 0.77 S cm^{-1}.[210] Similarly, a modified PilA sequence, in which the phenylalanine and tyrosine near the C-terminus of PilA were replaced by tryptophan, resulted in enhanced conductivity, with single nanofiber conductivities at least 500-fold greater than in the WT nanofibers.[224] This correlation between aromatic content and conductivity is also supported by comparisons of homologous nanofibers produced by other species in the *Geobacter* genus.[225] Nevertheless, the importance of aromatics does not constitute the presence of delocalized states. Reguera et al. have proposed that the aromatic amino acids instead function as discrete stepping stones for hopping.[217,222] Thus, the mechanism behind *G. sulfurreducens* pili remains a point of contention.[226]

π-Stacking has also been reported in a de novo peptide sequence composed entirely of natural amino acids, GFPRFAGFP.[227] This peptide, presented as a synthetic analogue to study *Geobacter* nanofiber conductivity, formed nanofibers that exhibited fluorescence spectra characteristic of π-stacking between phenylalanine side chains. In spite of the presence of π-stacking, the conductance of fiber films was low, $\sim 1 \times 10^{-11}$ S, albeit higher than conductances observed in amyloid β fibers.

4.3.2. Non-π-Stacked Peptides and Proteins. Although π-stacking is believed to play a critical role in the aforementioned examples of proteinogenic supramolecular conductors, it may not be necessary for long-range conduction through all peptide and protein materials. Despite affirmative evidence as to the significance of aromatic residues, most of the proposed *G. sulfurreducens* homology models do not support long-range electron delocalization via aromatic side-chain overlap.[226] The presence of aromatics may be critical to conduction, but delocalization via overlap may not be necessary and/or the only factor relevant to long-range conductivity.

This point is perhaps most clearly evident through a self-assembling de novo peptide sequence designed to form α-helical coiled coil hexamers with a supramolecular helical structure reminiscent of *Geobacter* nanofibers.[59] The core of these peptide nanofibers is rich in phenylalanine residues, yet the crystal structure of the hexamer indicates that the system is not π-stacked.[228] Phenyl rings in the hydrophobic core are in a canted orientation and too distant for π-orbital overlap, and no spectroscopic evidence was observed to support electronic delocalization. Nonetheless, single nanofiber fiber conductivities exceeded those measured for *Geobacter* nanofibers.[210,213] Bipotentiostatic measurements, which distinguish between redox-mediated and nonredox-mediated conduction,[145] reveal similar nonredox-mediated current responses for both the bacterial and the synthetic nanofibers. Additionally, both nanofiber systems exhibit a positive Arrhenius slope (S/K^{-1}) in buffer at physiologically relevant temperatures. This temperature dependence rules out a thermally activated mechanism at these temperatures but cannot be used to conclusively identify a precise conduction mechanism within the framework of known long-range conduction mechanisms. True metallic

DOI: 10.1021/acs.jpcb.8b07431
J. Phys. Chem. B 2018, 122, 10403−10423

conduction is unlikely, particularly due to the large band gap expected for peptides and in the absence of π-stacking delocalization. Although these studies do not identify a conduction mechanism, they demonstrate that an α-helical secondary structure and supramolecular ordering are determining factors for peptide conductivity in this system. They further show that conductivities comparable to conjugated polymers can be achieved in a non-π-stacked amino acid system.

The presence of aromatic residues alone may not be able to account for the high conductivity values observed in *Geobacter* and non-π-stacked peptide nanofibers. This point is clearly illustrated by the purely aromatic amino acid sequence, diphenylalanine (FF). Inspired by the β-amyloid polypeptide, FF is a minimal dipeptide known to form disparate nanostructures based on the choice of solvent.[229,230] Some self-assembly conditions result in porous nanotubular crystals, in which six interlocks, each composed of two linear diphenyls, surround an amide backbone "tube." The hydrogen bonds between the β-sheets forming these tubes participate in proton transfer and can exist either at the C or N terminus of strands between β-sheets. This configuration creates a double-well ground-state potential, which, in combination with the aromatic interlocks, reduces the band gaps to the semiconducting region. Regardless, conductance values remain low or insulating,[152,153] and the typical 4.7 Å distance between peptides may be too far to facilitate delocalization.[122,153]

Changing the bonding environment of the FF nanotubes directly impacts semiconducting properties. Current−voltage (I−V) measurements through nanotube networks demonstrated a fivefold increase in conductivity, from 0.3 to 1.6 nS upon replacing one of the phenylalanines in the dipeptide with a tryptophan[152] (Figure 9A,B), owing to a reduction of the molecular interstitial regions and proximity of aromatic overlap. This electronic change is supported by first-principles calculations, which show a reduction in nanotube bandgap from 4.48 to 3.04 eV upon switching from FF to FW[231] (Figure 9C). Changing the arrangement of the dipeptide within the nanotubes from the conventional hexagonal arrangement of linear diphenyls (linear FF) to a cyclic arrangement (cyclo-FF), in which the terminal carboxylic acid and amine groups fuse to form a cyclic amide backbone, also increases the I−V behavior from insulating to semiconducting due to better π-overlap in the cyclo-formation.[153] In this arrangement, the distance between phenylalanine residues is comparable to that of the non-π-stacked nanofiber;[59] nevertheless, unlike *Geobacter* nanofibers and the coiled-coil nanofibers, the cyclo-FF exhibits low conductances (~hundreds of pS) and a negative Arrhenius slope (S/K^{-1}). Conductivity in cyclo-FF may thus be thermally activated hopping between aromatic moieties or semiconducting transport with a narrowed band gap due to aromatic side-chain interactions.

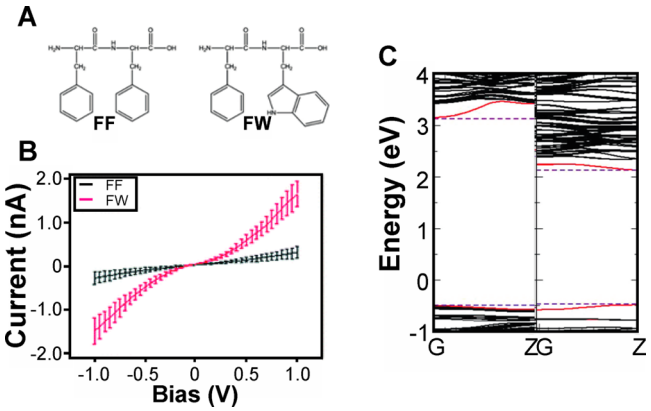

Figure 9. (A) Diphenylalnine (FF) and tryptophan-substituted (FW) peptides. (B) I−V characteristics of dipeptide fibrils. (C) Band structures along the tube axis for FF (left) and FW (right). The valence band maxima and conduction band minima are shown in red; dashed lines indicate the borders of the bandgaps. Adapted from Amdursky et al[152] and Akdim et al,[231] reproduced with permissions from the Royal Society of Chemistry copyright 2013 https://pubs.rsc.org/en/content/articlelanding/2013/cp/c3cp51748a#!divAbstract and the American Institute of Physics Publishing copyright 2015 https://aip.scitation.org/doi/abs/10.1063/1.4921012, respectively.

A separate class of proteinaceous bacterial appendages, known as curli, have been engineered to facilitate long-range conduction via aromatic amino acid redox hopping sites. Curli form aggregated amyloid fibers that are expressed on the surface of many Enterobacteriaceae, such as *Escherichia coli* and *Salmonella*.[232] These proteins derived from model organisms provide an experimental platform for developing conductive biological nanofibers.[58] The curlin fiber is composed of two structural proteins: a major subunit, CsgA, and a minor subunit, CsgB.[232−234,233] CsgA monomers have demonstrated robust fibrilization in a variety of in vitro conditions,[235,236] suggesting a tunable platform for synthetic modification. Seker and co-workers appended aromatic tripeptides, composed of tyrosine, tryptophan, histidine, or phenylalanine, onto the amyloidogenic region of the CsgA protein, R5T peptide.[58] They observed fiber assembly in all of the variants, with the tyrosine and tryptophan-modified R5T exhibiting the highest conductivity. These results informed subsequent experiments, in which they engineered tyrosine and tryptophan modifications to a CsgA fusion protein incorporating an 11 amino acid sequence borrowed from the *G. sulfurreducens* PilA protein (Section 4.3.1)[213,224] (Figure 10). *E. coli* biofilms expressing these modified CsgA proteins exhibited a 1.7- to 4-fold increase in conductivity relative to biofilms expressing WT CsgA. Seker et al. concluded from molecular structure models that, while CsgA fibers are not expected to form long-range π-stacked interactions, conduction is most likely facilitated through redox hopping along the side chains of tyrosine residues. While temperature-dependent conductivity data would be helpful in further supporting this claim, it is unclear whether the observed differences in conductance can be entirely attributed to the lowered redox potentials of tyrosine and tryptophan, since mutations to the CsgA sequence can produce differences in both film conductance and fiber morphology. Just as with the *Geobacter* nanofibers, additional structural information and complementary conductivity studies, such as temperature-dependent and single-fiber conductivity measurements, as well as spectroscopic investigations, are critical to supporting a specific conduction mechanism.

5. CONCLUSIONS AND OUTLOOK

Designing and understanding long-range (micrometer-scale) conduction through peptides and proteins is both fundamentally interesting and potentially significant for the development of bioelectronic materials. Herein, we have provided a detailed background of electron transport mechanisms pertinent to conduction along micrometer-scale supramolecular structures.

DOI: 10.1021/acs.jpcb.8b07431
J. Phys. Chem. B 2018, 122, 10403−10423

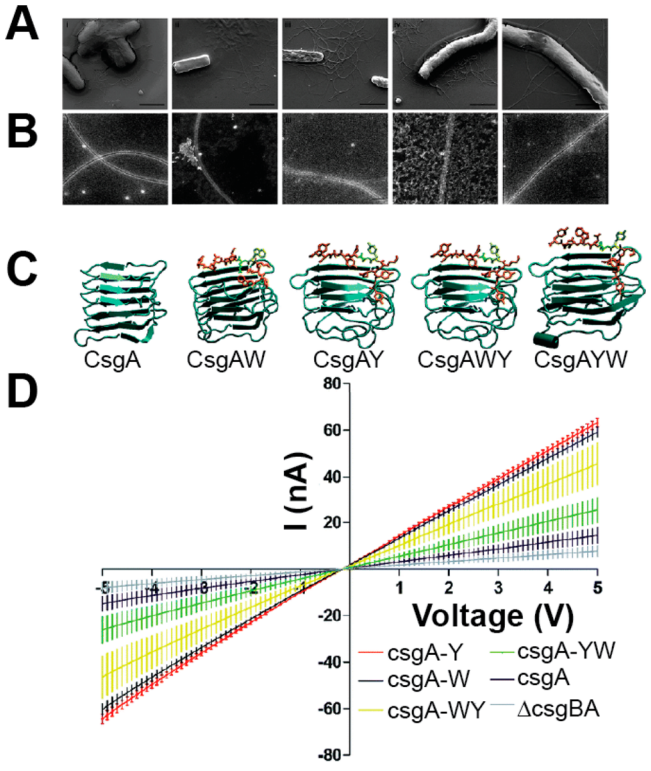

Figure 10. (A) Scanning and (B) transmission electron microscopy (TEM) images of the CsgA fibers and the designed conductive CsgA fibers produced by *E. coli* DcsgBA cells: (left to right) CsgA, CsgAW, CsgAY, CsgAWY, and CsgAYW. Diameters of the fibers from TEM were ∼12−15 nm, and many fibers came together to form thick fibrils. Scale bars are 2 μm for SEM (A) and 100 nm for TEM (B) images. (C) Molecular models of CsgA protein and its conductive motif-fused variants. (D) Output characteristics for CsgA and mutated CsgA proteins representing engineered amyloids fibers. Measurements were taken on three different electrodes for each sample. Curves represent the average of three independent samples. Adapted from Kalyoncu et al,[58] published by the Royal Society of Chemistry. Copyright 2017. https://pubs.rsc.org/en/content/articlelanding/2017/ra/c7ra06289c#!divAbstract

These transport mechanisms may be distinct from those governing short-range ET and ETp processes through single peptides and proteins on the nanometer-scale. Long-range conductivity has been demonstrated in cofactor-based and hybrid-peptide conjugate systems, as well as peptides and proteins with natural and unnatural amino acid side chains. While the redox principles behind long-range cofactor-based conduction can be clearly understood within the framework of an extended ET system, the emergence of long-range conductivity in noncofactor-based supramolecular systems remains an exciting research frontier.

Demonstrations of long-range conductivity in non-π-stacked peptide nanofibers and *G. sulfurreducens* nanofibers are particularly interesting, because they are orders of magnitude more conductive than optimally stacked hybrid organic peptide systems. Moreover, they suggest that π-stacking may not be necessary to achieve high, nonthermally activated conductivities in protein and peptide systems. Given the current structural information on these two systems, their conduction cannot entirely be explained by current long-range conduction models in peptide and proteins. The temperature-dependent conductivity measured in the bacterial fibers and the non-π-stacked nanofibers suggest a nonthermally activated transport mechanism, excluding both hopping and semiconducting models. However, metallic-like band conduction in a non-delocalized system, such as the non-π-stacked nanofibers, is highly unlikely. These two demonstrations thus suggest the need for additional structural characterization, such as cryo-EM, to verify the presence or absence of π-stacking and the supramolecular arrangements of these two fibers.

In general, the application of multiple complementary characterization techniques appears necessary to determining the dominant electronic conduction mechanisms in protein and peptide supramolecular materials. Their molecular dynamics are highly sensitive to different experimental conditions, and the chemical and structural components contributing to their conductivity, from cofactors to conjugated organic molecules to aromatic side chains, are capable of participating in several different mechanisms of conduction. Consequently, to better understand and improve this class of materials for bioelectronic applications, more comprehensive studies are required. To these ends, mutable building blocks, such as peptides and peptide conjugates, with robust self-assembly behavior, represent promising experimental platforms for systematic investigations of electronic conduction in amino acid-based materials. An improved understanding of how biology traffics electronic signals will pave the way for realizing the goal of bioelectronic materials to seamlessly integrate synthetic conductive materials with enzymes, cells, organs, and organisms.

AUTHOR INFORMATION

Corresponding Author

*E-mail: hochbaum@uci.edu. Phone: (949) 824-1194.

ORCID

Mohamed Y. El-Naggar: 0000-0001-5599-6309

Allon I. Hochbaum: 0000-0002-5377-8065

Notes

The authors declare no competing financial interest.

Biographies

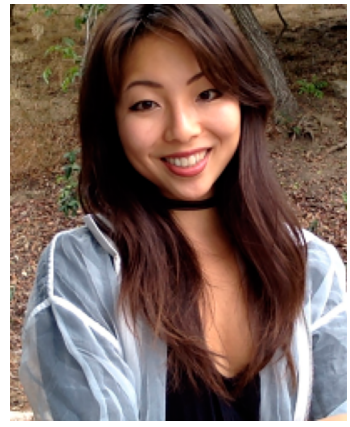

Nicole L. Ing obtained her Ph.D. in 2018 at the University of California, Irvine, studying biological and bioinspired electronic transport in supramolecular biomaterials under the supervision of Prof. Allon Hochbaum. She was a National Science Foundation Graduate Research Fellow and a Graduate Assistance in Areas of National Need Fellow. Ing received her B.A. in physics at Occidental College. Currently, she is a postdoctoral fellow of Sandia National Laboratories at the Joint BioEnergy Institute. Her research interests include electrochemistry, bioelectronics interfacing, and biomaterials.

DOI: 10.1021/acs.jpcb.8b07431
J. Phys. Chem. B 2018, 122, 10403−10423

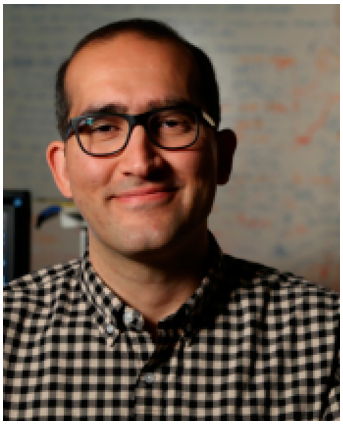

Moh El-Naggar is the Robert D. Beyer (1981) Early Career Chair in Natural Sciences, and Associate Professor of Physics, Biological Sciences, and Chemistry at the University of Southern California (USC). He received his B.S. degree from Lehigh University (2001), followed by M.S. (2002) and Ph.D. (2007) degrees from the California Institute of Technology, before doing his postdoctoral work at USC. El-Naggar's work is focused on charge transport and energy conversion at the interface between living cells and synthetic surfaces. His group has pioneered the development of new hybrid biotic/abiotic materials and renewable energy technologies that combine the exquisite biochemical control of nature with the synthetic building blocks of nanotechnology. El-Naggar was awarded the Presidential Early Career Award for Scientists and Engineers by President Obama in 2014, and he was named one of *Popular Science's* "Brilliant 10", and a Young Investigator Program Award from the Air Force Office of Scientific Research.

Allon Hochbaum is a Henry Samueli Early Career Assistant Professor in the Department of Chemical Engineering and Materials Science and the Department of Chemistry at the University of California, Irvine. He received a S.B. in Materials Science and Engineering from the Massachusetts Institute of Technology and completed his Ph.D. in the Department of Chemistry at UC Berkeley studying electrical and thermal transport phenomena in semiconductor nanowires. He was a postdoctoral research fellow at Harvard University, where he studied bacterial community dynamics at interfaces. Prof. Hochbaum is the recipient of the 3M Non-Tenured Faculty award, and the ACS (Division of Inorganic Chemistry) and AFOSR Young Investigator awards. His lab studies and designs electronically conductive natural and synthetic biomaterials and seeks to understand and engineer chemical signaling pathways involved in bacterial community development and antibiotic tolerance using chemical and physical approaches.

■ ACKNOWLEDGMENTS

M.E.-N.'s work on living electronics is supported by the Office of Naval Research Multidisciplinary University Research Initiative Grant No. N00014-15-1-2573. Work on microbial electron transfer in M.E.-N.'s laboratory is supported by Air Force Office of Scientific Research PECASE Award No. FA9550-14-1-0294 (nanoscale characterization of electron transport networks) and the Division of Chemical Sciences, Geosciences, and Biosciences, Office of Basic Energy Sciences of the U.S. Department of Energy through Grant No. DE-FG02-13ER16415. Work by N.L.I. and A.I.H. on electrical conductivity in natural and synthetic supramolecular biomaterials is supported by the Air Force Office of Scientific Research Award No. FA9550-14-1-0350 and National Science Foundation Award No. CHE-1808143. N.L.I. was supported while preparing this review by a U.S. Department of Education G.A.A.N.N. fellowship.

■ REFERENCES

(1) Milroy, C. A.; Manthiram, A. Bioelectronic Energy Storage: A Pseudocapacitive Hydrogel Composed of Endogenous Biomolecules. *ACS Energy Lett* **2016**, *1* (4), 672−677.

(2) Abdellaoui, S.; Chavez, M. S.; Matanovic, I.; Stephens, A. R.; Atanassov, P.; Minteer, S. D. Hybrid Molecular/Enzymatic Catalytic Cascade for Complete Electro-Oxidation of Glycerol Using a Promiscuous NAD-Dependent Formate Dehydrogenase from Candida Boidinii. *Chem. Commun.* **2017**, *53* (39), 5368−5371.

(3) Song, R.-B.; Wu, Y.; Lin, Z.-Q.; Xie, J.; Tan, C. H.; Loo, J. S. C.; Cao, B.; Zhang, J.-R.; Zhu, J.-J.; Zhang, Q. Living and Conducting: Coating Individual Bacterial Cells with In Situ Formed Polypyrrole. *Angew. Chem., Int. Ed.* **2017**, *56* (35), 10516−10520.

(4) Lee, S.; Peh, W. Y. X.; Wang, J.; Yang, F.; Ho, J. S.; Thakor, N. V.; Yen, S.; Lee, C. Toward Bioelectronic Medicine—Neuromodulation of Small Peripheral Nerves Using Flexible Neural Clip. *Adv. Sci.* **2017**, *4* (11), 1700149.

(5) Koopman, F. A.; Chavan, S. S.; Miljko, S.; Grazio, S.; Sokolovic, S.; Schuurman, P. R.; Mehta, A. D.; Levine, Y. A.; Faltys, M.; Zitnik, R.; et al. Vagus Nerve Stimulation Inhibits Cytokine Production and Attenuates Disease Severity in Rheumatoid Arthritis. *Proc. Natl. Acad. Sci. U. S. A.* **2016**, *113* (29), 8284−8289.

(6) Mishra, S.; Norton, J. J. S.; Lee, Y.; Lee, D. S.; Agee, N.; Chen, Y.; Chun, Y.; Yeo, W.-H. Soft, Conformal Bioelectronics for a Wireless Human-Wheelchair Interface. *Biosens. Bioelectron.* **2017**, *91*, 796−803.

(7) Tasca, F.; Gorton, L.; Kujawa, M.; Patel, I.; Harreither, W.; Peterbauer, C. K.; Ludwig, R.; Nöll, G. Increasing the Coulombic Efficiency of Glucose Biofuel Cell Anodes by Combination of Redox Enzymes. *Biosens. Bioelectron.* **2010**, *25* (7), 1710−1716.

(8) Tanabe, Y.; Ho, J. S.; Liu, J.; Liao, S.-Y.; Zhen, Z.; Hsu, S.; Shuto, C.; Zhu, Z.-Y.; Ma, A.; Vassos, C.; et al. High-Performance Wireless Powering for Peripheral Nerve Neuromodulation Systems. *PLoS One* **2017**, *12* (10), e0186698.

(9) Han, S.; Kim, J.; Won, S. M.; Ma, Y.; Kang, D.; Xie, Z.; Lee, K.-T.; Chung, H. U.; Banks, A.; Min, S.; et al. Battery-Free, Wireless Sensors for Full-Body Pressure and Temperature Mapping. *Sci. Transl. Med.* **2018**, *10* (435), eaan4950.

(10) Choi, J.; Ghaffari, R.; Baker, L. B.; Rogers, J. A. Skin-Interfaced Systems for Sweat Collection and Analytics. *Sci. Adv.* **2018**, *4* (2), eaar3921.

(11) Xu, L.; Gutbrod, S. R.; Bonifas, A. P.; Su, Y.; Sulkin, M. S.; Lu, N.; Chung, H.-J.; Jang, K.-I.; Liu, Z.; Ying, M.; et al. 3D Multifunctional Integumentary Membranes for Spatiotemporal Cardiac Measurements and Stimulation across the Entire Epicardium. *Nat. Commun.* **2014**, *5*, 3329.

(12) Capogrosso, M.; Milekovic, T.; Borton, D.; Wagner, F.; Moraud, E. M.; Mignardot, J.-B.; Buse, N.; Gandar, J.; Barraud, Q.;

DOI: 10.1021/acs.jpcb.8b07431
J. Phys. Chem. B 2018, 122, 10403−10423

Xing, D.; et al. A Brain−spine Interface Alleviating Gait Deficits after Spinal Cord Injury in Primates. *Nature* **2016**, *539* (7628), 284−288.
(13) Mastinu, E.; Doguet, P.; Botquin, Y.; Hakansson, B.; Ortiz-Catalan, M. Embedded System for Prosthetic Control Using Implanted Neuromuscular Interfaces Accessed Via an Osseointegrated Implant. *IEEE Trans. Biomed. Circuits Syst.* **2017**, *11* (4), 867−877.
(14) Ciancio, A. L.; Cordella, F.; Barone, R.; Romeo, R. A.; Bellingegni, A. D.; Sacchetti, R.; Davalli, A.; Di Pino, G.; Ranieri, F.; Di Lazzaro, V.; et al. Control of Prosthetic Hands via the Peripheral Nervous System. *Front. Neurosci.* **2016**, *10*, 116.
(15) Chuang, M.-C.; Windmiller, J. R.; Santhosh, P.; Ramírez, G. V.; Katz, E.; Wang, J. High-Fidelity Determination of Security Threats via a Boolean Biocatalytic Cascade. *Chem. Commun.* **2011**, *47* (11), 3087−3089.
(16) Duncan, B.; Le, N. D. B.; Alexander, C.; Gupta, A.; Yesilbag Tonga, G.; Yazdani, M.; Landis, R. F.; Wang, L.-S.; Yan, B.; Burmaoglu, S.; et al. Sensing by Smell: Nanoparticle−Enzyme Sensors for Rapid and Sensitive Detection of Bacteria with Olfactory Output. *ACS Nano* **2017**, *11* (6), 5339−5343.
(17) Lu, Y.; Li, H.; Zhuang, S.; Zhang, D.; Zhang, Q.; Zhou, J.; Dong, S.; Liu, Q.; Wang, P. Olfactory Biosensor Using Odorant-Binding Proteins from Honeybee: Ligands of Floral Odors and Pheromones Detection by Electrochemical Impedance. *Sens. Actuators, B* **2014**, *193*, 420−427.
(18) Xie, X.; Ye, M.; Hsu, P.-C.; Liu, N.; Criddle, C. S.; Cui, Y. Microbial Battery for Efficient Energy Recovery. *Proc. Natl. Acad. Sci. U. S. A.* **2013**, *110* (40), 15925−15930.
(19) Pant, D.; Singh, A.; van Bogaert, G.; Olsen, S. I.; Nigam, P. S.; Diels, L.; Vanbroekhoven, K. Bioelectrochemical Systems (BES) for Sustainable Energy Production and Product Recovery from Organic Wastes and Industrial Wastewaters. *RSC Adv.* **2012**, *2* (4), 1248−1263.
(20) Bornscheuer, U. T.; Huisman, G. W.; Kazlauskas, R. J.; Lutz, S.; Moore, J. C.; Robins, K. Engineering the Third Wave of Biocatalysis. *Nature* **2012**, *485* (7397), 185−194.
(21) Kataoka, M.; Miyakawa, T.; Shimizu, S.; Tanokura, M. Enzymes Useful for Chiral Compound Synthesis: Structural Biology, Directed Evolution, and Protein Engineering for Industrial Use. *Appl. Microbiol. Biotechnol.* **2016**, *100* (13), 5747−5757.
(22) Kim, D.-H.; Ghaffari, R.; Lu, N.; Rogers, J. A. Flexible and Stretchable Electronics for Biointegrated Devices. *Annu. Rev. Biomed. Eng.* **2012**, *14*, 113−128.
(23) Wang, S.; Li, M.; Wu, J.; Kim, D.-H.; Lu, N.; Su, Y.; Kang, Z.; Huang, Y.; Rogers, J. A. Mechanics of Epidermal Electronics. *J. Appl. Mech.* **2012**, *79* (3), 31022.
(24) Heary, R. F.; Parvathreddy, N.; Sampath, S.; Agarwal, N. Elastic Modulus in the Selection of Interbody Implants. *J. Spine Surg.* **2017**, *3* (2), 163−167.
(25) Hanefeld, U.; Gardossi, L.; Magner, E. Understanding Enzyme Immobilisation. *Chem. Soc. Rev.* **2009**, *38* (2), 453−468.
(26) Vasylieva, N.; Maucler, C.; Meiller, A.; Viscogliosi, H.; Lieutaud, T.; Barbier, D.; Marinesco, S. Immobilization Method to Preserve Enzyme Specificity in Biosensors: Consequences for Brain Glutamate Detection. *Anal. Chem.* **2013**, *85* (4), 2507−2515.
(27) Mohamad, N. R.; Marzuki, N. H. C.; Buang, N. A.; Huyop, F.; Wahab, R. A. An Overview of Technologies for Immobilization of Enzymes and Surface Analysis Techniques for Immobilized Enzymes. *Biotechnol. Biotechnol. Equip.* **2015**, *29* (2), 205−220.
(28) Agostini, F.; Völler, J.-S.; Koksch, B.; Acevedo-Rocha, C. G.; Kubyshkin, V.; Budisa, N. Biocatalysis with Unnatural Amino Acids: Enzymology Meets Xenobiology. *Angew. Chem., Int. Ed.* **2017**, *56* (33), 9680−9703.
(29) Young, T. S.; Schultz, P. G. Beyond the Canonical 20 Amino Acids: Expanding the Genetic Lexicon. *J. Biol. Chem.* **2010**, *285* (15), 11039−11044.
(30) Wang, L.; Xie, J.; Schultz, P. G. Expanding the Genetic Code. *Annu. Rev. Biophys. Biomol. Struct.* **2006**, *35*, 225−249.
(31) Ravikumar, Y.; Nadarajan, S. P.; Hyeon Yoo, T.; Lee, C.-S.; Yun, H. Incorporating Unnatural Amino Acids to Engineer Biocatalysts for Industrial Bioprocess Applications. *Biotechnol. J.* **2015**, *10* (12), 1862−1876.
(32) Zelzer, M.; Todd, S. J.; Hirst, A. R.; McDonald, T. O.; Ulijn, R. V. Enzyme Responsive Materials: Design Strategies and Future Developments. *Biomater. Sci.* **2013**, *1* (1), 11−39.
(33) Kumar, M.; Ing, N. L.; Narang, V.; Wijerathne, N. K.; Hochbaum, A. I.; Ulijn, R. V. Amino-Acid-Encoded Biocatalytic Self-Assembly Enables the Formation of Transient Conducting Nanostructures. *Nat. Chem.* **2018**, *10*, 696−703.
(34) Brown, J. E.; Moreau, J. E.; Berman, A. M.; McSherry, H. J.; Coburn, J. M.; Schmidt, D. F.; Kaplan, D. L. Shape Memory Silk Protein Sponges for Minimally Invasive Tissue Regeneration. *Adv. Healthcare Mater.* **2017**, *6* (2), 1600762.
(35) Bayrak, A.; Prüger, P.; Stock, U. A.; Seifert, M. Absence of Immune Responses with Xenogeneic Collagen and Elastin. *Tissue Eng., Part A* **2013**, *19* (13−14), 1592−1600.
(36) DeLustro, F.; Dasch, J.; Keefe, J.; Ellingsworth, L. Immune Responses to Allogeneic and Xenogeneic Implants of Collagen and Collagen Derivatives. *Clin. Orthop. Relat. Res.* **1990**, *260*, 263−279.
(37) Turabee, M. H.; Thambi, T.; Lym, J. S.; Lee, D. S. Bioresorbable Polypeptide-Based Comb-Polymers Efficiently Improves the Stability and Pharmacokinetics of Proteins in Vivo. *Biomater. Sci.* **2017**, *5* (4), 837−848.
(38) Tao, H.; Hwang, S.-W.; Marelli, B.; An, B.; Moreau, J. E.; Yang, M.; Brenckle, M. A.; Kim, S.; Kaplan, D. L.; Rogers, J. A.; et al. Silk-Based Resorbable Electronic Devices for Remotely Controlled Therapy and in Vivo Infection Abatement. *Proc. Natl. Acad. Sci. U. S. A.* **2014**, *111* (49), 17385−17389.
(39) Rajkhowa, R.; Hu, X.; Tsuzuki, T.; Kaplan, D. L.; Wang, X. Structure and Biodegradation Mechanism of Milled Bombyx Mori Silk Particles. *Biomacromolecules* **2012**, *13* (8), 2503−2512.
(40) Giano, M. C.; Pochan, D. J.; Schneider, J. P. Controlled Biodegradation of Self-Assembling β-Hairpin Peptide Hydrogels by Proteolysis with Matrix Metalloproteinase-13. *Biomaterials* **2011**, *32* (27), 6471−6477.
(41) Shi, J.; Schellinger, J. G.; Pun, S. H. Engineering Biodegradable and Multifunctional Peptide-Based Polymers for Gene Delivery. *J. Biol. Eng.* **2013**, *7*, 25.
(42) Fu, J.; Reinhold, J.; Woodbury, N. W. Peptide-Modified Surfaces for Enzyme Immobilization. *PLoS One* **2011**, *6* (4), e18692.
(43) Fu, J.; Cai, K.; Johnston, S. A.; Woodbury, N. W. Exploring Peptide Space for Enzyme Modulators. *J. Am. Chem. Soc.* **2010**, *132* (18), 6419−6424.
(44) Wei, G.; Wang, L.; Dong, D.; Teng, Z.; Shi, Z.; Wang, K.; An, G.; Guan, Y.; Han, B.; Yao, M.; et al. Promotion of Cell Growth and Adhesion of a Peptide Hydrogel Scaffold via mTOR/Cadherin Signaling. *J. Cell. Physiol.* **2018**, *233* (2), 822−829.
(45) Dong, D.-m.; Wei, G.-j.; Wang, Y.-S.; Zhou, C.-W.; Wan, D.-Y.; Lei, P.-Z.; Wen, J.; Lei, H.-W.; Dong, D.-M. Promotion of Peripheral Nerve Regeneration of a Peptide Compound Hydrogel Scaffold. *Int. J. Nanomed.* **2013**, *8*, 3217−3225.
(46) Wang, X.; Qiao, L.; Horii, A. Screening of Functionalized Self-Assembling Peptide Nanofiber Scaffolds with Angiogenic Activity for Endothelial Cell Growth. *Prog. Nat. Sci.* **2011**, *21* (2), 111−116.
(47) De Santis, E.; Ryadnov, M. G. Peptide Self-Assembly for Nanomaterials: The Old New Kid on the Block. *Chem. Soc. Rev.* **2015**, *44* (22), 8288−8300.
(48) Bai, Y.; Luo, Q.; Liu, J. Protein Self-Assembly via Supramolecular Strategies. *Chem. Soc. Rev.* **2016**, *45* (10), 2756−2767.
(49) Liu, J.; Xie, C.; Dai, X.; Jin, L.; Zhou, W.; Lieber, C. M. Multifunctional Three-Dimensional Macroporous Nanoelectronic Networks for Smart Materials. *Proc. Natl. Acad. Sci. U. S. A.* **2013**, *110* (17), 6694−6699.
(50) Duan, X.; Gao, R.; Xie, P.; Cohen-Karni, T.; Qing, Q.; Choe, H. S.; Tian, B.; Jiang, X.; Lieber, C. M. Intracellular Recordings of Action Potentials by an Extracellular Nanoscale Field-Effect Transistor. *Nat. Nanotechnol.* **2012**, *7* (3), 174−179.

DOI: 10.1021/acs.jpcb.8b07431
J. Phys. Chem. B 2018, 122, 10403−10423

(51) Parviz, B. A.; Ryan, D.; Whitesides, G. M. Using Self-Assembly for the Fabrication of Nano-Scale Electronic and Photonic Devices. *IEEE Trans. Adv. Packag.* **2003**, *26* (3), 233−241.
(52) Ron, I.; Pecht, I.; Sheves, M.; Cahen, D. Proteins as Solid-State Electronic Conductors. *Acc. Chem. Res.* **2010**, *43* (7), 945−953.
(53) Bostick, C. D.; Mukhopadhyay, S.; Pecht, I.; Sheves, M.; Cahen, D.; Lederman, D. Protein Bioelectronics: A Review of What We Do and Do Not Know. *Rep. Prog. Phys.* **2018**, *81* (2), 26601.
(54) Edwards, P. P.; Gray, H. B.; Lodge, M. T. J.; Williams, R. J. P. Electron Transfer and Electronic Conduction through an Intervening Medium. *Angew. Chem., Int. Ed.* **2008**, *47* (36), 6758−6765.
(55) Xu, H.; Das, A. K.; Horie, M.; Shaik, M. S.; Smith, A. M.; Luo, Y.; Lu, X.; Collins, R.; Liem, S. Y.; Song, A.; et al. An Investigation of the Conductivity of Peptide Nanotube Networks Prepared by Enzyme-Triggered Self-Assembly. *Nanoscale* **2010**, *2* (6), 960−966.
(56) Ardoña, H. A. M.; Besar, K.; Togninalli, M.; Katz, H. E.; Tovar, J. D. Sequence-Dependent Mechanical, Photophysical and Electrical Properties of Pi-Conjugated Peptide Hydrogelators. *J. Mater. Chem. C* **2015**, *3* (25), 6505−6514.
(57) Malvankar, N. S.; Vargas, M.; Nevin, K. P.; Franks, A. E.; Leang, C.; Kim, B.-C.; Inoue, K.; Mester, T.; Covalla, S. F.; Johnson, J. P.; et al. Tunable Metallic-like Conductivity in Microbial Nanowire Networks. *Nat. Nanotechnol.* **2011**, *6* (9), 573−579.
(58) Kalyoncu, E.; Ahan, R. E.; Olmez, T. T.; Seker, U. O. S. Genetically Encoded Conductive Protein Nanofibers Secreted by Engineered Cells. *RSC Adv.* **2017**, *7* (52), 32543−32551.
(59) Ing, N. L.; Spencer, R. K.; Luong, S. H.; Nguyen, H. D.; Hochbaum, A. I. Electronic Conductivity in Biomimetic α-Helical Peptide Nanofibers and Gels. *ACS Nano* **2018**, *12* (3), 2652−2661.
(60) Panda, S. S.; Katz, H. E.; Tovar, J. D. Solid-State Electrical Applications of Protein and Peptide Based Nanomaterials. *Chem. Soc. Rev.* **2018**, *47* (10), 3640−3658.
(61) Winkler, J. R.; Gray, H. B. Long-Range Electron Tunneling. *J. Am. Chem. Soc.* **2014**, *136* (8), 2930−2939.
(62) Gray, H. B.; Winkler, J. R. Long-Range Electron Transfer. *Proc. Natl. Acad. Sci. U. S. A.* **2005**, *102* (10), 3534−3539.
(63) Blumberger, J. Recent Advances in the Theory and Molecular Simulation of Biological Electron Transfer Reactions. *Chem. Rev.* **2015**, *115* (20), 11191−11238.
(64) Shah, A.; Adhikari, B.; Martic, S.; Munir, A.; Shahzad, S.; Ahmad, K.; Kraatz, H.-B. Electron Transfer in Peptides. *Chem. Soc. Rev.* **2015**, *44* (4), 1015−1027.
(65) Amdursky, N. Electron Transfer across Helical Peptides. *ChemPlusChem* **2015**, *80* (7), 1075−1095.
(66) Williamson, H. R.; Dow, B. A.; Davidson, V. L. Mechanisms for Control of Biological Electron Transfer Reactions. *Bioorg. Chem.* **2014**, *57*, 213−221.
(67) Amdursky, N.; Marchak, D.; Sepunaru, L.; Pecht, I.; Sheves, M.; Cahen, D. Electronic Transport via Proteins. *Adv. Mater.* **2014**, *26* (42), 7142−7161.
(68) Venkatramani, R.; Wierzbinski, E.; Waldeck, D. H.; Beratan, D. N. Breaking the Simple Proportionality between Molecular Conductances and Charge Transfer Rates. *Faraday Discuss.* **2014**, *174*, 57−78.
(69) Wierzbinski, E.; Venkatramani, R.; Davis, K. L.; Bezer, S.; Kong, J.; Xing, Y.; Borguet, E.; Achim, C.; Beratan, D. N.; Waldeck, D. H. The Single-Molecule Conductance and Electrochemical Electron-Transfer Rate Are Related by a Power Law. *ACS Nano* **2013**, *7* (6), 5391−5401.
(70) Skourtis, S. S. Review: Probing Protein Electron Transfer Mechanisms from the Molecular to the Cellular Length Scales. *Biopolymers* **2013**, *100* (1), 82−92.
(71) Marcus, R. A. On the Theory of Oxidation-Reduction Reactions Involving Electron Transfer. I. *J. Chem. Phys.* **1956**, *24* (5), 966−978.
(72) Marcus, R. A. Electrostatic Free Energy and Other Properties of States Having Nonequilibrium Polarization. I. *J. Chem. Phys.* **1956**, *24* (5), 979−989.
(73) Page, C. C.; Moser, C. C.; Chen, X.; Dutton, P. L. Natural Engineering Principles of Electron Tunnelling in Biological Oxidation−reduction. *Nature* **1999**, *402* (6757), 47−52.
(74) Beratan, D. N.; Betts, J. N.; Onuchic, J. N. Protein Electron Transfer Rates Set by the Bridging Secondary and Tertiary Structure. *Science* **1991**, *252* (5010), 1285−1288.
(75) Stuchebrukhov, A. A. Tunneling Currents in Electron Transfer Reactions in Proteins. *J. Chem. Phys.* **1996**, *104* (21), 8424−8432.
(76) Langen, R.; Colón, J. L.; Casimiro, D. R.; Karpishin, T. B.; Winkler, J. R.; Gray, H. B. Electron Tunneling in Proteins: Role of the Intervening Medium. *JBIC, J. Biol. Inorg. Chem.* **1996**, *1* (3), 221−225.
(77) Jones, M. L.; Kurnikov, I. V.; Beratan, D. N. The Nature of Tunneling Pathway and Average Packing Density Models for Protein-Mediated Electron Transfer. *J. Phys. Chem. A* **2002**, *106* (10), 2002−2006.
(78) Gray, H. B.; Winkler, J. R. Electron Flow through Proteins. *Chem. Phys. Lett.* **2009**, *483* (1−3), 1−9.
(79) Hines, T.; Diez-Perez, I.; Hihath, J.; Liu, H.; Wang, Z.-S.; Zhao, J.; Zhou, G.; Müllen, K.; Tao, N. Transition from Tunneling to Hopping in Single Molecular Junctions by Measuring Length and Temperature Dependence. *J. Am. Chem. Soc.* **2010**, *132* (33), 11658−11664.
(80) Gray, H. B.; Winkler, J. R. Electron Tunneling through Proteins. *Q. Rev. Biophys.* **1999**, *36* (3), 341−372.
(81) Skourtis, S. S.; Balabin, I. A.; Kawatsu, T.; Beratan, D. N. Protein Dynamics and Electron Transfer: Electronic Decoherence and Non-Condon Effects. *Proc. Natl. Acad. Sci. U. S. A.* **2005**, *102* (10), 3552−3557.
(82) Zhang, Y.; Liu, C.; Balaeff, A.; Skourtis, S. S.; Beratan, D. N. Biological Charge Transfer via Flickering Resonance. *Proc. Natl. Acad. Sci. U. S. A.* **2014**, *111* (28), 10049−10054.
(83) Beratan, D. N.; Liu, C.; Migliore, A.; Polizzi, N. F.; Skourtis, S. S.; Zhang, P.; Zhang, Y. Charge Transfer in Dynamical Biosystems, or The Treachery of (Static) Images. *Acc. Chem. Res.* **2015**, *48* (2), 474−481.
(84) Giese, B.; Graber, M.; Cordes, M. Electron Transfer in Peptides and Proteins. *Curr. Opin. Chem. Biol.* **2008**, *12* (6), 755−759.
(85) Miller, A.; Abrahams, E. Impurity Conduction at Low Concentrations. *Phys. Rev.* **1960**, *120* (3), 745−755.
(86) Morigaki, K. *Physics of Amorphous Semiconductors;* Imperial College Press: London, U.K., 1999.
(87) Mott, N. F. Conduction in Non-Crystalline Materials. *Philos. Mag.* **1969**, *19* (160), 835−852.
(88) Davis, E. A.; Mott, N. F. Conduction in Non-Crystalline Systems V. Conductivity, Optical Absorption and Photoconductivity in Amorphous Semiconductors. *Philos. Mag.* **1970**, *22* (179), 0903−0922.
(89) Renger, T.; Marcus, R. A. Variable-Range Hopping Electron Transfer through Disordered Bridge States: Application to DNA. *J. Phys. Chem. A* **2003**, *107* (41), 8404−8419.
(90) Taniguchi, V. T.; Sailasuta-Scott, N.; Anson, F. C.; Gray, H. B. Thermodynamics of Metalloprotein Electron Transfer Reactions. *Pure Appl. Chem.* **1980**, *52* (10), 2275−2281.
(91) Warren, J. J.; Winkler, J. R.; Gray, H. B. Redox Properties of Tyrosine and Related Molecules. *FEBS Lett.* **2012**, *586* (5), 596−602.
(92) Cordes, M.; et al. Influence of Amino Acid Side Chains on Long-Distance Electron Transfer in Peptides: Electron Hopping via "Stepping Stones.". *Angew. Chem., Int. Ed.* **2008**, *47* (18), 3461−3463.
(93) Giese, B.; Wang, M.; Gao, J.; Stoltz, M.; Müller, P.; Graber, M. Electron Relay Race in Peptides. *J. Org. Chem.* **2009**, *74* (10), 3621−3625.
(94) Harriman, A. Further Comments on the Redox Potentials of Tryptophan and Tyrosine. *J. Phys. Chem.* **1987**, *91* (24), 6102−6104.
(95) Navaratnam, S.; Parsons, B. J. Reduction Potential of Histidine Free Radicals: A Pulse Radiolysis Study. *J. Chem. Soc., Faraday Trans.* **1998**, *94* (17), 2577−2581.
(96) Morozova, O. B.; Yurkovskaya, A. V. Intramolecular Electron Transfer in the Photooxidized Peptides Tyrosine−Histidine and

DOI: 10.1021/acs.jpcb.8b07431
J. Phys. Chem. B 2018, 122, 10403−10423

Histidine−Tyrosine: A Time-Resolved CIDNP Study. *Angew. Chem., Int. Ed.* **2010**, *49* (43), 7996−7999.
(97) Nathanael, J. G.; Wille, U.; Gamon, L.; Cordes, M.; Rablen, P.; Bally, T.; Fromm, K.; Giese, B. Amide Neighbouring Group Effects in Peptides: Phenylalanine as Relay Amino Acid in Long-Distance Electron Transfer. *ChemBioChem* **2018**, *19* (9), 922−926.
(98) Ener, M. E.; Gray, H. B.; Winkler, J. R. Hole Hopping through Tryptophan in Cytochrome P450. *Biochemistry* **2017**, *56* (28), 3531−3538.
(99) Dempsey, J. L.; Winkler, J. R.; Gray, H. B. Proton-Coupled Electron Flow in Protein Redox Machines. *Chem. Rev.* **2010**, *110* (12), 7024−7039.
(100) Zhao, X. G.; Cukier, R. I. Molecular Dynamics and Quantum Chemistry Study of a Proton-Coupled Electron Transfer Reaction. *J. Phys. Chem.* **1995**, *99* (3), 945−954.
(101) Zhang, M.-T.; Hammarström, L. Proton-Coupled Electron Transfer from Tryptophan: A Concerted Mechanism with Water as Proton Acceptor. *J. Am. Chem. Soc.* **2011**, *133* (23), 8806−8809.
(102) Polizzi, N. F.; Migliore, A.; Therien, M. J.; Beratan, D. N. Defusing Redox Bombs? *Proc. Natl. Acad. Sci. U. S. A.* **2015**, *112* (35), 10821−10822.
(103) Gray, H. B.; Winkler, J. R. Hole Hopping through Tyrosine/Tryptophan Chains Protects Proteins from Oxidative Damage. *Proc. Natl. Acad. Sci. U. S. A.* **2015**, *112* (35), 10920−10925.
(104) Dalton, E. F.; Surridge, N. A.; Jernigan, J. C.; Wilbourn, K. O.; Facci, J. S.; Murray, R. W. Charge Transport in Electroactive Polymers Consisting of Fixed Molecular Redox Sites. *Chem. Phys.* **1990**, *141* (1), 143−157.
(105) Akhoury, A.; Bromberg, L.; Hatton, T. A. Interplay of Electron Hopping and Bounded Diffusion during Charge Transport in Redox Polymer Electrodes. *J. Phys. Chem. B* **2013**, *117* (1), 333−342.
(106) Forster, R. J.; Walsh, D. A.; Mano, N.; Mao, F.; Heller, A. Modulating the Redox Properties of an Osmium-Containing Metallopolymer through the Supporting Electrolyte and Cross-Linking. *Langmuir* **2004**, *20* (3), 862−868.
(107) Snider, R. M.; Strycharz-Glaven, S. M.; Tsoi, S. D.; Erickson, J. S.; Tender, L. M. Long-Range Electron Transport in Geobacter Sulfurreducens Biofilms Is Redox Gradient-Driven. *Proc. Natl. Acad. Sci. U. S. A.* **2012**, *109* (38), 15467−15472.
(108) Strycharz-Glaven, S. M.; Snider, R. M.; Guiseppi-Elie, A.; Tender, L. M. On the Electrical Conductivity of Microbial Nanowires and Biofilms. *Energy Environ. Sci.* **2011**, *4* (11), 4366−4379.
(109) Yates, M. D.; Barr Engel, S.; Eddie, B. J.; Lebedev, N.; Malanoski, A. P.; Tender, L. M. Redox-Gradient Driven Electron Transport in a Mixed Community Anodic Biofilm. *FEMS Microbiol. Ecol.* **2018**, *94* (6), fiy081.
(110) Subramanian, P.; Pirbadian, S.; El-Naggar, M. Y.; Jensen, G. J. Ultrastructure of Shewanella Oneidensis MR-1 Nanowires Revealed by Electron Cryotomography. *Proc. Natl. Acad. Sci. U. S. A.* **2018**, *115* (14), E3246−E3255.
(111) Blauch, D. N.; Saveant, J. M. Dynamics of Electron Hopping in Assemblies of Redox Centers. Percolation and Diffusion. *J. Am. Chem. Soc.* **1992**, *114* (9), 3323−3332.
(112) Lu, N.; Banerjee, W.; Sun, P.; Gao, N.; Liu, M.; et al. Charge Carrier Hopping Transport Based on Marcus Theory and Variable-Range Hopping Theory in Organic Semiconductors. *J. Appl. Phys.* **2015**, *118* (4), 45701.
(113) Endres, R. G.; Cox, D. L.; Singh, R. R. P. Colloquium: The Quest for High-Conductance DNA. *Rev. Mod. Phys.* **2004**, *76* (1), 195−214.
(114) Tao, K.; Makam, P.; Aizen, R.; Gazit, E. Self-Assembling Peptide Semiconductors. *Science* **2017**, *358* (6365), eaam9756.
(115) Evans, M. G.; Gergely, J. A Discussion of the Possibility of Bands of Energy Levels in Proteins Electronic Interaction in Non Bonded Systems. *Biochim. Biophys. Acta* **1949**, *3*, 188−197.
(116) Ladik, J. Energy Band Structure of Proteins. *Nature* **1964**, *202*, 1208−1209.
(117) Orton, J. W.; Powell, M. J. The Hall Effect in Polycrystalline and Powdered Semiconductors. *Rep. Prog. Phys.* **1980**, *43* (11), 1263.
(118) Horowitz, G.; Hajlaoui, M. E.; Hajlaoui, R. Temperature and Gate Voltage Dependence of Hole Mobility in Polycrystalline Oligothiophene Thin Film Transistors. *J. Appl. Phys.* **2000**, *87* (9), 4456−4463.
(119) Matsui, H.; Kumaki, D.; Takahashi, E.; Takimiya, K.; Tokito, S.; Hasegawa, T. Correlation between Interdomain Carrier Hopping and Apparent Mobility in Polycrystalline Organic Transistors as Investigated by Electron Spin Resonance. *Phys. Rev. B: Condens. Matter Mater. Phys.* **2012**, *85* (3), 35308.
(120) Chelli, R.; Gervasio, F. L.; Procacci, P.; Schettino, V. Stacking and T-Shape Competition in Aromatic−Aromatic Amino Acid Interactions. *J. Am. Chem. Soc.* **2002**, *124* (21), 6133−6143.
(121) McGaughey, G. B.; Gagné, M.; Rappé, A. K. π-Stacking Interactions. Alive and Well in Proteins. *J. Biol. Chem.* **1998**, *273* (25), 15458−15463.
(122) Takahashi, R.; Wang, H.; Lewis, J. P. Electronic Structures and Conductivity in Peptide Nanotubes. *J. Phys. Chem. B* **2007**, *111* (30), 9093−9098.
(123) Sepunaru, L.; Refaely-Abramson, S.; Lovrinčić, R.; Gavrilov, Y.; Agrawal, P.; Levy, Y.; Kronik, L.; Pecht, I.; Sheves, M.; Cahen, D. Electronic Transport via Homopeptides: The Role of Side Chains and Secondary Structure. *J. Am. Chem. Soc.* **2015**, *137* (30), 9617−9626.
(124) Guo, C.; Yu, X.; Refaely-Abramson, S.; Sepunaru, L.; Bendikov, T.; Pecht, I.; Kronik, L.; Vilan, A.; Sheves, M.; Cahen, D. Tuning Electronic Transport via Hepta-Alanine Peptides Junction by Tryptophan Doping. *Proc. Natl. Acad. Sci. U. S. A.* **2016**, *113* (39), 10785−10790.
(125) Issa, J. B.; Krogh-Jespersen, K.; Isied, S. S. Conformational Dependence of Electronic Coupling Across Peptide Bonds: A Ramachandran Map. *J. Phys. Chem. C* **2010**, *114* (48), 20809−20812.
(126) Minnihan, E. C.; Nocera, D. G.; Stubbe, J. Reversible, Long-Range Radical Transfer in E. Coli Class Ia Ribonucleotide Reductase. *Acc. Chem. Res.* **2013**, *46* (11), 2524−2535.
(127) Larsson, A.; Sjöberg, B. M. Identification of the Stable Free Radical Tyrosine Residue in Ribonucleotide Reductase. *EMBO J.* **1986**, *5* (8), 2037−2040.
(128) Costentin, C. Electrochemical Approach to the Mechanistic Study of Proton-Coupled Electron Transfer. *Chem. Rev.* **2008**, *108* (7), 2145−2179.
(129) Barry, B. A. Reaction Dynamics and Proton Coupled Electron Transfer: Studies of Tyrosine-Based Charge Transfer in Natural and Biomimetic Systems. *Biochim. Biophys. Acta, Bioenerg.* **2015**, *1847* (1), 46−54.
(130) Xiao, X.; Xu, B.; Tao, N. Conductance Titration of Single-Peptide Molecules. *J. Am. Chem. Soc.* **2004**, *126* (17), 5370−5371.
(131) Gao, J.; Müller, P.; Wang, M.; Eckhardt, S.; Lauz, M.; Fromm, K. M.; Giese, B. Electron Transfer in Peptides: The Influence of Charged Amino Acids - Gao - 2011 - Angewandte Chemie International Edition - Wiley Online Library. *Angew. Chem., Int. Ed.* **2011**, *50* (8), 1926−1930.
(132) Shin, Y. K.; Newton, M. D.; Isied, S. S. Distance Dependence of Electron Transfer Across Peptides with Different Secondary Structures: The Role of Peptide Energetics and Electronic Coupling. *J. Am. Chem. Soc.* **2003**, *125* (13), 3722−3732.
(133) Galoppini, E.; Fox, M. A. Effect of the Electric Field Generated by the Helix Dipole on Photoinduced Intramolecular Electron Transfer in Dichromophoric α-Helical Peptides. *J. Am. Chem. Soc.* **1996**, *118* (9), 2299−2300.
(134) Fox, M. A.; Galoppini, E. Electric Field Effects on Electron Transfer Rates in Dichromophoric Peptides: The Effect of Helix Unfolding. *J. Am. Chem. Soc.* **1997**, *119* (23), 5277−5285.
(135) Lauz, M.; Eckhardt, S.; Fromm, K. M.; Giese, B. The Influence of Dipole Moments on the Mechanism of Electron Transfer through Helical Peptides. *Phys. Chem. Chem. Phys.* **2012**, *14* (40), 13785−13788.
(136) Chen, X.; Zhang, L.; Zhang, L.; Sun, W.; Zhang, Z.; Liu, H.; Bu, Y.; Cukier, R. I. α-Helix C-Terminus Acting as a Relay to Mediate Long-Range Hole Migration in Proteins. *J. Phys. Chem. Lett.* **2010**, *1* (10), 1637−1641.

DOI: 10.1021/acs.jpcb.8b07431
J. Phys. Chem. B 2018, 122, 10403−10423

(137) Crofts, A. R.; Wraight, C. A. The Electrochemical Domain of Photosynthesis. *Biochim. Biophys. Acta, Rev. Bioenerg.* **1983**, *726* (3), 149−185.
(138) Rochaix, J.-D. Regulation of Photosynthetic Electron Transport. *Biochim. Biophys. Acta, Bioenerg.* **2011**, *1807* (3), 375−383.
(139) Zickermann, V.; Kerscher, S.; Zwicker, K.; Tocilescu, M. A.; Radermacher, M.; Brandt, U. Architecture of Complex I and Its Implications for Electron Transfer and Proton Pumping. *Biochim. Biophys. Acta, Bioenerg.* **2009**, *1787* (6), 574−583.
(140) Cecchini, G. Function and Structure of Complex II of the Respiratory Chain. *Annu. Rev. Biochem.* **2003**, *72*, 77−109.
(141) Bond, D. R.; Lovley, D. R. Electricity Production by Geobacter Sulfurreducens Attached to Electrodes. *Appl. Environ. Microbiol.* **2003**, *69* (3), 1548−1555.
(142) Malvankar, N. S.; Tuominen, M. T.; Lovley, D. R. Biofilm Conductivity Is a Decisive Variable for High-Current-Density Geobacter Sulfurreducens Microbial Fuel Cells. *Energy Environ. Sci.* **2012**, *5* (2), 5790−5797.
(143) Leang, C.; Malvankar, N. S.; Franks, A. E.; Nevin, K. P.; Lovley, D. R. Engineering Geobacter Sulfurreducens to Produce a Highly Cohesive Conductive Matrix with Enhanced Capacity for Current Production. *Energy Environ. Sci.* **2013**, *6* (6), 1901−1908.
(144) Yates, M. D.; Strycharz-Glaven, S. M.; Golden, J. P.; Roy, J.; Tsoi, S.; Erickson, J. S.; El-Naggar, M. Y.; Barton, S. C.; Tender, L. M. Measuring Conductivity of Living Geobacter Sulfurreducens Biofilms. *Nat. Nanotechnol.* **2016**, *11* (11), 910−913.
(145) Ing, N. L.; Nusca, T. D.; Hochbaum, A. I. Geobacter Sulfurreducens Pili Support Ohmic Electronic Conduction in Aqueous Solution. *Phys. Chem. Chem. Phys.* **2017**, *19* (32), 21791−21799.
(146) Robuschi, L.; Tomba, J. P.; Schrott, G. D.; Bonanni, P.; Desimone, P.; Busalmen, J. P. Spectroscopic Slicing to Reveal Internal Redox Gradients in Electricity-Producing Biofilms. *Angew. Chem., Int. Ed.* **2013**, *52* (3), 925−928.
(147) Burgess, M.; Moore, J. S.; Rodriguez-López, J. Redox Active Polymers as Soluble Nanomaterials for Energy Storage. *Acc. Chem. Res.* **2016**, *49* (11), 2649−2657.
(148) Park, H.-S.; Ko, S.-J.; Park, J.-S.; Kim, J. Y.; Song, H.-K. Redox-Active Charge Carriers of Conducting Polymers as a Tuner of Conductivity and Its Potential Window. *Sci. Rep.* **2013**, *3*, 2454.
(149) Altamura, L.; Horvath, C.; Rengaraj, S.; Rongier, A.; Elouarzaki, K.; Gondran, C.; Maçon, A. L. B.; Vendrely, C.; Bouchiat, V.; Fontecave, M.; et al. A Synthetic Redox Biofilm Made from Metalloprotein−prion Domain Chimera Nanowires. *Nat. Chem.* **2017**, *9* (2), 157−163.
(150) Wang, J.; Li, D.; Yang, M.; Zhang, Y. A Novel Ferrocene-Tagged Peptide Nanowire for Enhanced Electrochemical Glucose Biosensing. *Anal. Methods* **2014**, *6* (18), 7161−7165.
(151) Yemini, M.; Reches, M.; Rishpon, J.; Gazit, E. Novel Electrochemical Biosensing Platform Using Self-Assembled Peptide Nanotubes. *Nano Lett.* **2005**, *5* (1), 183−186.
(152) Amdursky, N. Enhanced Solid-State Electron Transport via Tryptophan Containing Peptide Networks. *Phys. Chem. Chem. Phys.* **2013**, *15* (32), 13479−13482.
(153) Lee, J. S.; Yoon, I.; Kim, J.; Ihee, H.; Kim, B.; Park, C. B. Self-Assembly of Semiconducting Photoluminescent Peptide Nanowires in the Vapor Phase. *Angew. Chem., Int. Ed.* **2011**, *50* (5), 1164−1167.
(154) Rowe, A. R.; Rajeev, P.; Jain, A.; Pirbadian, S.; Okamoto, A.; Gralnick, J. A.; El-Naggar, M. Y.; Nealson, K. H. Tracking Electron Uptake from a Cathode into Shewanella Cells: Implications for Energy Acquisition from Solid-Substrate Electron Donors. *mBio* **2018**, *9* (1), e02203−17.
(155) Prakash, G. K. S.; Viva, F. A.; Bretschger, O.; Yang, B.; El-Naggar, M.; Nealson, K. Inoculation Procedures and Characterization of Membrane Electrode Assemblies for Microbial Fuel Cells. *J. Power Sources* **2010**, *195* (1), 111−117.
(156) Clarke, T. A.; Edwards, M. J.; Gates, A. J.; Hall, A.; White, G. F.; Bradley, J.; Reardon, C. L.; Shi, L.; Beliaev, A. S.; Marshall, M. J.; et al. Structure of a Bacterial Cell Surface Decaheme Electron Conduit. *Proc. Natl. Acad. Sci. U. S. A.* **2011**, *108* (23), 9384−9389.
(157) El-Naggar, M. Y.; Wanger, G.; Leung, K. M.; Yuzvinsky, T. D.; Southam, G.; Yang, J.; Lau, W. M.; Nealson, K. H.; Gorby, Y. A. Electrical Transport along Bacterial Nanowires from Shewanella Oneidensis MR-1. *Proc. Natl. Acad. Sci. U. S. A.* **2010**, *107* (42), 18127−18131.
(158) Pirbadian, S.; Barchinger, S. E.; Leung, K. M.; Byun, H. S.; Jangir, Y.; Bouhenni, R. A.; Reed, S. B.; Romine, M. F.; Saffarini, D. A.; Shi, L.; et al. Shewanella Oneidensis MR-1 Nanowires Are Outer Membrane and Periplasmic Extensions of the Extracellular Electron Transport Components. *Proc. Natl. Acad. Sci. U. S. A.* **2014**, *111* (35), 12883−12888.
(159) Leung, K. M.; Wanger, G.; El-Naggar, M. Y.; Gorby, Y.; Southam, G.; Lau, W. M.; Yang, J. Shewanella Oneidensis MR-1 Bacterial Nanowires Exhibit P-Type, Tunable Electronic Behavior. *Nano Lett.* **2013**, *13* (6), 2407−2411.
(160) Xu, S.; Barrozo, A.; Tender, L. M.; Krylov, A. I.; El-Naggar, M. Y. Multiheme Cytochrome Mediated Redox Conduction through Shewanella Oneidensis MR-1 Cells. *J. Am. Chem. Soc.* **2018**, *140* (32), 10085−10089.
(161) Yi, H. T.; Gartstein, Y. N.; Podzorov, V. Charge Carrier Coherence and Hall Effect in Organic Semiconductors. *Sci. Rep.* **2016**, *6*, 23650.
(162) Fleming, S.; Ulijn, R. V. Design of Nanostructures Based on Aromatic Peptide Amphiphiles. *Chem. Soc. Rev.* **2014**, *43* (23), 8150−8177.
(163) Diegelmann, S. R.; Gorham, J. M.; Tovar, J. D. One-Dimensional Optoelectronic Nanostructures Derived from the Aqueous Self-Assembly of π-Conjugated Oligopeptides. *J. Am. Chem. Soc.* **2008**, *130* (42), 13840−13841.
(164) Kumar, R. J.; MacDonald, J. M.; Singh, T. B.; Waddington, L. J.; Holmes, A. B. Hierarchical Self-Assembly of Semiconductor Functionalized Peptide α-Helices and Optoelectronic Properties. *J. Am. Chem. Soc.* **2011**, *133* (22), 8564−8573.
(165) Stone, D. A.; Hsu, L.; Stupp, S. I. Self-Assembling Quinquethiophene−Oligopeptide Hydrogelators. *Soft Matter* **2009**, *5* (10), 1990−1993.
(166) Klok, H.-A.; Rösler, A.; Götz, G.; Mena-Osteritz, E.; Bäuerle, P. Synthesis of a Silk-Inspired Peptide − Oligothiophene Conjugate. *Org. Biomol. Chem.* **2004**, *2* (24), 3541−3544.
(167) Pandeeswar, M.; Khare, H.; Ramakumar, S.; Govindaraju, T. Crystallographic Insight-Guided Nanoarchitectonics and Conductivity Modulation of an N-Type Organic Semiconductor through Peptide Conjugation. *Chem. Commun.* **2015**, *51* (39), 8315−8318.
(168) Nalluri, S. K. M.; Berdugo, C.; Javid, N.; Frederix, P. W. J. M.; Ulijn, R. V. Biocatalytic Self-Assembly of Supramolecular Charge-Transfer Nanostructures Based on n-Type Semiconductor-Appended Peptides. *Angew. Chem., Int. Ed.* **2014**, *53* (23), 5882−5887.
(169) Vadehra, G. S.; Wall, B. D.; Diegelmann, S. R.; Tovar, J. D. On-Resin Dimerization Incorporates a Diverse Array of π-Conjugated Functionality within Aqueous Self-Assembling Peptide Backbones. *Chem. Commun.* **2010**, *46* (22), 3947−3949.
(170) Eakins, G. L.; Gallaher, J. K.; Keyzers, R. A.; Falber, A.; Webb, J. E. A.; Laos, A.; Tidhar, Y.; Weissman, H.; Rybtchinski, B.; Thordarson, P.; et al. Thermodynamic Factors Impacting the Peptide-Driven Self-Assembly of Perylene Diimide Nanofibers. *J. Phys. Chem. B* **2014**, *118* (29), 8642−8651.
(171) Eakins, G. L.; Pandey, R.; Wojciechowski, J. P.; Zheng, H. Y.; Webb, J. E. A.; Valéry, C.; Thordarson, P.; Plank, N. O. V.; Gerrard, J. A.; Hodgkiss, J. M. Functional Organic Semiconductors Assembled via Natural Aggregating Peptides. *Adv. Funct. Mater.* **2015**, *25* (35), 5640−5649.
(172) Marty, R.; Szilluweit, R.; Sánchez-Ferrer, A.; Bolisetty, S.; Adamcik, J.; Mezzenga, R.; Spitzner, E.-C.; Feifer, M.; Steinmann, S. N.; Corminboeuf, C.; et al. Hierarchically Structured Microfibers of "Single Stack" Perylene Bisimide and Quaterthiophene Nanowires. *ACS Nano* **2013**, *7* (10), 8498−8508.

DOI: 10.1021/acs.jpcb.8b07431
J. Phys. Chem. B 2018, 122, 10403−10423

(173) Draper, E. R.; Walsh, J. J.; McDonald, T. O.; Zwijnenburg, M. A.; Cameron, P. J.; Cowan, A. J.; Adams, D. J. Air-Stable Photoconductive Films Formed from Perylene Bisimide Gelators. *J. Mater. Chem. C* **2014**, *2* (28), 5570−5575.
(174) Draper, E. R.; Greeves, B. J.; Barrow, M.; Schweins, R.; Zwijnenburg, M. A.; Adams, D. J. pH-Directed Aggregation to Control Photoconductivity in Self-Assembled Perylene Bisimides. *Chem* **2017**, *2* (5), 716−731.
(175) Smith, A. M.; Williams, R. J.; Tang, C.; Coppo, P.; Collins, R. F.; Turner, M. L.; Saiani, A.; Ulijn, R. V. Fmoc-Diphenylalanine Self Assembles to a Hydrogel via a Novel Architecture Based on Π−π Interlocked β-Sheets. *Adv. Mater.* **2008**, *20* (1), 37−41.
(176) Draper, E. R.; Morris, K. L.; Little, M. A.; Raeburn, J.; Colquhoun, C.; Cross, E. R.; McDonald, T. O.; Serpell, L. C.; Adams, D. J. Hydrogels Formed from Fmoc Amino Acids. *CrystEngComm* **2015**, *17* (42), 8047−8057.
(177) Kim, S.; Parquette, J. A Model for the Controlled Assembly of Semiconductor Peptides. *Nanoscale* **2012**, *4* (22), 6940−6947.
(178) Wall, B. D.; Zacca, A. E.; Sanders, A. M.; Wilson, W. L.; Ferguson, A. L.; Tovar, J. D. Supramolecular Polymorphism: Tunable Electronic Interactions within π-Conjugated Peptide Nanostructures Dictated by Primary Amino Acid Sequence. *Langmuir* **2014**, *30* (20), 5946−5956.
(179) Birks, J. B. Excimers. *Rep. Prog. Phys.* **1975**, *38*, 903−974.
(180) Hartgerink, J. D.; Granja, J. R.; Milligan, R. A.; Ghadiri, M. R. Self-Assembling Peptide Nanotubes. *J. Am. Chem. Soc.* **1996**, *118* (1), 43−50.
(181) Channon, K. J.; Devlin, G. L.; Magennis, S. W.; Finlayson, C. E.; Tickler, A. K.; Silva, C.; MacPhee, C. E. Modification of Fluorophore Photophysics through Peptide-Driven Self-Assembly. *J. Am. Chem. Soc.* **2008**, *130* (16), 5487−5491.
(182) Vandermeulen, G. W. M.; Klok, H.-A. Peptide/Protein Hybrid Materials: Enhanced Control of Structure and Improved Performance through Conjugation of Biological and Synthetic Polymers. *Macromol. Biosci.* **2004**, *4* (4), 383−398.
(183) Wall, B. D.; Diegelmann, S. R.; Zhang, S.; Dawidczyk, T. J.; Wilson, W. L.; Katz, H. E.; Mao, H.-Q.; Tovar, J. D. Aligned Macroscopic Domains of Optoelectronic Nanostructures Prepared via Shear-Flow Assembly of Peptide Hydrogels. *Adv. Mater.* **2011**, *23* (43), 5009−5014.
(184) Besar, K.; Ardoña, H. A. M.; Tovar, J. D.; Katz, H. E. Demonstration of Hole Transport and Voltage Equilibration in Self-Assembled π-Conjugated Peptide Nanostructures Using Field-Effect Transistor Architectures. *ACS Nano* **2015**, *9* (12), 12401−12409.
(185) Diegelmann, S. R.; Hartman, N.; Markovic, N.; Tovar, J. D. Synthesis and Alignment of Discrete Polydiacetylene-Peptide Nanostructures. *J. Am. Chem. Soc.* **2012**, *134* (4), 2028−2031.
(186) Sanders, A. M.; Dawidczyk, T. J.; Katz, H. E.; Tovar, J. D. Peptide-Based Supramolecular Semiconductor Nanomaterials via Pd-Catalyzed Solid-Phase "Dimerizations.". *ACS Macro Lett.* **2012**, *1* (11), 1326−1329.
(187) Nakano, K.; Iino, H.; Usui, T.; Hanna, J. Bulk Mobility of Polycrystalline Thin Films of Quaterthiophene Derivatives. *Appl. Phys. Lett.* **2011**, *98* (10), 103302.
(188) Nalluri, S. K. M.; Shivarova, N.; Kanibolotsky, A. L.; Zelzer, M.; Gupta, S.; Frederix, P. W. J. M.; Skabara, P. J.; Gleskova, H.; Ulijn, R. V. Conducting Nanofibers and Organogels Derived from the Self-Assembly of Tetrathiafulvalene-Appended Dipeptides. *Langmuir* **2014**, *30* (41), 12429−12437.
(189) Das, A. K.; Collins, R.; Ulijn, R. V. Exploiting Enzymatic (Reversed) Hydrolysis in Directed Self-Assembly of Peptide Nanostructures. *Small* **2008**, *4* (2), 279−287.
(190) Xu, H.; Das, A. K.; Horie, M.; Shaik, M. S.; Smith, A. M.; Luo, Y.; Lu, X.; Collins, R.; Liem, S. Y.; Song, A.; et al. An Investigation of the Conductivity of Peptide Nanotube Networks Prepared by Enzyme-Triggered Self-Assembly. *Nanoscale* **2010**, *2* (6), 960−966.
(191) Zhu, J.; Dexheimer, M.; Cheng, H. Reconfigurable Systems for Multifunctional Electronics. *Npj Flex. Electron.* **2017**, *1* (1), 8.
(192) Carloni, P.; Andreoni, W.; Parrinello, M. Self-Assembled Peptide Nanotubes from First Principles. *Phys. Rev. Lett.* **1997**, *79* (4), 761−764.
(193) Jishi, R. A.; et al. Peptide Nanotubes: An Inert Environment. *Phys. Rev. B: Condens. Matter Mater. Phys.* **1998**, *58* (24), R16009−R16011.
(194) Okamoto, H.; Nakanishi, T.; Nagai, Y.; Kasahara, M.; Takeda, K. Variety of the Molecular Conformation in Peptide Nanorings and Nanotubes. *J. Am. Chem. Soc.* **2003**, *125* (9), 2756−2769.
(195) Ashkenasy, N.; Horne, W. S.; Ghadiri, M. Design of Self-Assembling Peptide Nanotubes with Delocalized Electronic States. *Small* **2006**, *2* (1), 99−102.
(196) Horne, W. S.; Ashkenasy, N.; Ghadiri, M. R. Modulating Charge Transfer through Cyclic D,L-Alpha-Peptide Self-Assembly. *Chem. - Eur. J.* **2005**, *11* (4), 1137−1144.
(197) Montenegro, J.; Ghadiri, M. R.; Granja, J. R. Ion Channel Models Based on Self-Assembling Cyclic Peptide Nanotubes. *Acc. Chem. Res.* **2013**, *46* (12), 2955−2965.
(198) Yardeni, J. L.; Amit, M.; Ashkenasy, G.; Ashkenasy, N. Sequence Dependent Proton Conduction in Self-Assembled Peptide Nanostructures. *Nanoscale* **2016**, *8* (4), 2358−2366.
(199) Weber, J.; Senior, A. E. ATP Synthesis Driven by Proton Transport in F1F0-ATP Synthase. *FEBS Lett.* **2003**, *545* (1), 61−70.
(200) Luecke, H.; Richter, H. T.; Lanyi, J. K. Proton Transfer Pathways in Bacteriorhodopsin at 2.3 Angstrom Resolution. *Science* **1998**, *280* (5371), 1934−1937.
(201) Heberle, J. Proton Transfer Reactions across Bacteriorhodopsin and along the Membrane. *Biochim. Biophys. Acta, Bioenerg.* **2000**, *1458* (1), 135−147.
(202) Sineshchekov, O. A.; Govorunova, E. G.; Wang, J.; Li, H.; Spudich, J. L. Intramolecular Proton Transfer in Channelrhodopsins. *Biophys. J.* **2013**, *104* (4), 807−817.
(203) Miyake, T.; Rolandi, M. Grotthuss Mechanisms: From Proton Transport in Proton Wires to Bioprotonic Devices. *J. Phys.: Condens. Matter* **2016**, *28* (2), 23001.
(204) Meng, X.; Wang, H.-N.; Song, S.-Y.; Zhang, H.-J. Proton-Conducting Crystalline Porous Materials. *Chem. Soc. Rev.* **2017**, *46* (2), 464−480.
(205) Deng, Y.; Josberger, E.; Jin, J.; Roudsari, A. F.; Helms, B. A.; Zhong, C.; Anantram, M. P.; Rolandi, M. H+-Type and OH−-Type Biological Protonic Semiconductors and Complementary Devices. *Sci. Rep.* **2013**, *3*, 2481.
(206) Ivnitski, D.; Amit, M.; Rubinov, B.; Cohen-Luria, R.; Ashkenasy, N.; Ashkenasy, G. Introducing Charge Transfer Functionality into Prebiotically Relevant β-Sheet Peptide Fibrils. *Chem. Commun.* **2014**, *50* (51), 6733−6736.
(207) Amit, M.; Cheng, G.; Hamley, I. W.; Ashkenasy, N. Conductance of Amyloid β Based Peptide Filaments: Structure−Function Relations. *Soft Matter* **2012**, *8* (33), 8690−8696.
(208) Amit, M.; Appel, S.; Cohen, R.; Cheng, G.; Hamley, I. W.; Ashkenasy, N. Hybrid Proton and Electron Transport in Peptide Fibrils. *Adv. Funct. Mater.* **2014**, *24* (37), 5873−5880.
(209) Malvankar, N. S.; Vargas, M.; Nevin, K.; Tremblay, P.-L.; Evans-Lutterodt, K.; Nykypanchuk, D.; Martz, E.; Tuominen, M. T.; Lovley, D. R. Structural Basis for Metallic-like Conductivity in Microbial Nanowires. *mBio* **2015**, *6* (2), e00084−15.
(210) Lampa-Pastirk, S.; Veazey, J. P.; Walsh, K. A.; Feliciano, G. T.; Steidl, R. J.; Tessmer, S. H.; Reguera, G. Thermally Activated Charge Transport in Microbial Protein Nanowires. *Sci. Rep.* **2016**, *6*, 23517.
(211) Malvankar, N. S.; Tuominen, M. T.; Lovley, D. R.; Strycharz-Glaven, S. M.; Snider, R. M.; Guiseppi-Elie, A.; Tender, L. M. Comment on "On Electrical Conductivity of Microbial Nanowires and Biofilms". *Energy Environ. Sci* **2011**, *4*, 4366. *Energy Environ. Sci.* **2012**, *5* (3), 6247−6249.
(212) Strycharz-Glaven, S. M.; Tender, L. M.; Malvankar, N. S.; Tuominen, M. T.; Lovley, D. R. Reply to the "Comment on 'On Electrical Conductivity of Microbial Nanowires and Biofilms'". *Energy Environ. Sci* **2012**, *5*, 6250−6255, DOI: 10.1039/c2ee02613a.

DOI: 10.1021/acs.jpcb.8b07431
J. Phys. Chem. B 2018, 122, 10403−10423

(213) Adhikari, R. Y.; Malvankar, N. S.; Tuominen, M. T.; Lovley, D. R. Conductivity of Individual Geobacter Pili. *RSC Adv.* **2016**, *6* (10), 8354−8357.
(214) Reardon, P. N.; Mueller, K. T. Structure of the Type IVa Major Pilin from the Electrically Conductive Bacterial Nanowires of Geobacter Sulfurreducens. *J. Biol. Chem.* **2013**, *288* (41), 29260−29266.
(215) Chang, Y.-W.; Rettberg, L. A.; Treuner-Lange, A.; Iwasa, J.; Søgaard-Andersen, L.; Jensen, G. J. Architecture of the Type IVa Pilus Machine. *Science* **2016**, *351* (6278), aad2001−aad2007.
(216) Ing, N. L.; Nusca, T. D.; Hochbaum, A. I. Geobacter Sulfurreducens Pili Support Ohmic Electronic Conduction in Aqueous Solution. *Phys. Chem. Chem. Phys.* **2017**, *19*, 21791.
(217) Steidl, R. J.; Lampa-Pastirk, S.; Reguera, G. Mechanistic Stratification in Electroactive Biofilms of Geobacter Sulfurreducens Mediated by Pilus Nanowires. *Nat. Commun.* **2016**, *7*, 12217.
(218) Kaiser, A. B. Systematic Conductivity Behavior in Conducting Polymers: Effects of Heterogeneous Disorder. *Adv. Mater.* **2001**, *13* (12−13), 927−941.
(219) Xiao, K.; Malvankar, N. S.; Shu, C.; Martz, E.; Lovley, D. R.; Sun, X. Low Energy Atomic Models Suggesting a Pilus Structure That Could Account for Electrical Conductivity of Geobacter Sulfurreducens Pili. *Sci. Rep.* **2016**, *6*, 23385.
(220) Vargas, M.; Malvankar, N. S.; Tremblay, P.-L.; Leang, C.; Smith, J. A.; Patel, P.; Synoeyenbos-West, O.; Nevin, K. P.; Lovley, D. R. Aromatic Amino Acids Required for Pili Conductivity and Long-Range Extracellular Electron Transport in Geobacter Sulfurreducens. *mBio* **2013**, *4* (2), e00105−e00113.
(221) Boesen, T.; Nielsen, L. P. Molecular Dissection of Bacterial Nanowires. *mBio* **2013**, *4* (3), e00270−13.
(222) Feliciano, G. T.; Steidl, R. J.; Reguera, G. Structural and Functional Insights into the Conductive Pili of Geobacter Sulfurreducens Revealed in Molecular Dynamics Simulations. *Phys. Chem. Chem. Phys.* **2015**, *17* (34), 22217−22226.
(223) Feliciano, G. T.; da Silva, A. J. R.; Reguera, G.; Artacho, E. Molecular and Electronic Structure of the Peptide Subunit of Geobacter Sulfurreducens Conductive Pili from First Principles. *J. Phys. Chem. A* **2012**, *116* (30), 8023−8030.
(224) Tan, Y.; Adhikari, R. Y.; Malvankar, N. S.; Pi, S.; Ward, J. E.; Woodard, T. L.; Nevin, K. P.; Xia, Q.; Tuominen, M. T.; Lovley, D. R. Synthetic Biological Protein Nanowires with High Conductivity. *Small* **2016**, *12* (33), 4481−4485.
(225) Tan, Y.; Adhikari, R. Y.; Malvankar, N. S.; Ward, J. E.; Woodard, T. L.; Nevin, K. P.; Lovley, D. R. Expressing the Geobacter Metallireducens PilA in Geobacter Sulfurreducens Yields Pili with Exceptional Conductivity. *mBio* **2017**, *8* (1). DOI: 10.1128/mBio.02203-16
(226) Creasey, R. C. G.; Mostert, A. B.; Nguyen, T. A. H.; Virdis, B.; Freguia, S.; Laycock, B. Microbial Nanowires − Electron Transport and the Role of Synthetic Analogues. *Acta Biomater.* **2018**, *69*, 1−30.
(227) Creasey, R. C. G.; Shingaya, Y.; Nakayama, T. Improved Electrical Conductance through Self-Assembly of Bioinspired Peptides into Nanoscale Fibers. *Mater. Chem. Phys.* **2015**, *158*, 52−59.
(228) Spencer, R. K.; Hochbaum, A. I. X-Ray Crystallographic Structure and Solution Behavior of an Antiparallel Coiled-Coil Hexamer Formed by de Novo Peptides. *Biochemistry* **2016**, *55* (23), 3214−3223.
(229) Zhu, P.; Yan, X.; Su, Y.; Yang, Y.; Li, J. Solvent-Induced Structural Transition of Self-Assembled Dipeptide: From Organogels to Microcrystals. *Chem. - Eur. J.* **2010**, *16* (10), 3176−3183.
(230) Mason, T. O.; Chirgadze, D. Y.; Levin, A.; Adler-Abramovich, L.; Gazit, E.; Knowles, T. P. J.; Buell, A. K. Expanding the Solvent Chemical Space for Self-Assembly of Dipeptide Nanostructures. *ACS Nano* **2014**, *8* (2), 1243−1253.
(231) Akdim, B.; Pachter, R.; Naik, R. R. Self-Assembled Peptide Nanotubes as Electronic Materials: An Evaluation from First-Principles Calculations. *Appl. Phys. Lett.* **2015**, *106* (18), 183707.
(232) Barnhart, M. M.; Chapman, M. R. Curli Biogenesis and Function. *Annu. Rev. Microbiol.* **2006**, *60*, 131−147.
(233) Hammer, N. D.; Schmidt, J. C.; Chapman, M. R. The Curli Nucleator Protein, CsgB, Contains an Amyloidogenic Domain That Directs CsgA Polymerization. *Proc. Natl. Acad. Sci. U. S. A.* **2007**, *104* (30), 12494−12499.
(234) Bian, Z.; Normark, S. Nucleator Function of CsgB for the Assembly of Adhesive Surface Organelles in Escherichia Coli. *EMBO J.* **1997**, *16* (19), 5827−5836.
(235) Chapman, M. R.; Robinson, L. S.; Pinkner, J. S.; Roth, R.; Heuser, J.; Hammar, M.; Normark, S.; Hultgren, S. J. Role of Escherichia Coli Curli Operons in Directing Amyloid Fiber Formation. *Science* **2002**, *295* (5556), 851−855.
(236) Dueholm, M. S.; Nielsen, S. B.; Hein, K. L.; Nissen, P.; Chapman, M.; Christiansen, G.; Nielsen, P. H.; Otzen, D. E. Fibrillation of the Major Curli Subunit CsgA under a Wide Range of Conditions Implies a Robust Design of Aggregation. *Biochemistry* **2011**, *50* (39), 8281−8290.

DOI: 10.1021/acs.jpcb.8b07431
J. Phys. Chem. B 2018, 122, 10403−10423